

# Structures and trends of neutral $\text{MX}_x\text{solvent}_{4-x}$ tetrahedra and anionic $[\text{MX}_4]^{2-}$ tetrahalometallates of zinc(II), cadmium(II) and mercury(II) with benzopyridine- and benzopyrazine-type N-donor ligands or cations†

C. Slabbert and M. Rademeyer \*

Department of Chemistry, University of Pretoria, cnr Lynnwood Road & Roper Street, Hatfield, Pretoria 0002, South Africa

## Abstract

Zinc, cadmium and mercury dihalides were reacted with benzopyridine- and benzopyrazine-type N-donor molecules acridine (acr), phenazine (phe), quinoline (quin) and quinoxaline (quinox) as ligands or cations. The solid-state structures of 16 novel, zero-dimensional reaction products were studied by X-ray diffraction. Seven of the compounds were prepared in the presence of an inorganic acid, HX, which resulted in the formation of anionic tetrahalometallates,  $[\text{MX}_4]^{2-}$ , with either  $\text{Cd}^{2+}$  or  $\text{Hg}^{2+}$  as the cationic metal center and quinolinium (quin-H), quinoxalinium (quinox-H), acridinium (acr-H) or phenazinium (phe-H) as the counter cation. The other nine compounds contain  $\text{Zn}^{2+}$  as the tetrahedral cationic node. Five of the nine  $\text{Zn}^{2+}$  compounds are neutral, and four are ionic. Three of the four ionic  $\text{Zn}^{2+}$  compounds contain an anionic tetrahalometallate inorganic moiety,  $[\text{ZnX}_4]^{2-}$ , while the inorganic component of the fourth ionic  $\text{Zn}^{2+}$  compound is coordinated by three halido ligands and one aqua ligand,  $[\text{ZnX}_3(\text{H}_2\text{O})]^-$ . Structural trends, hydrogen bonding interactions and aromatic interactions are identified. In addition, it is observed that in the case of the neutral phenazine or acridine compounds, the size of the organic molecule prevents coordination of the molecule to the metal ion.

## Introduction

In 2011, Bowmaker et al.<sup>1</sup> conducted a structural and spectroscopic study on an inclusive range of neutral  $\text{ML}_2\text{X}_2$  adducts formed between group 12 metal halides,  $\text{MX}_2$  ( $\text{M} = \text{Zn}^{2+}$ ,  $\text{Cd}^{2+}$  and  $\text{X} = \text{Cl}^-$ ,  $\text{Br}^-$ ,  $\text{I}^-$ ), and the pyridine- and benzopyridine-type N-donor ligands pyridine, 2-methylpyridine, 2,4,6-trimethylpyridine and quinoline. Towards the synthesis of halide-bridged polymers of the divalent group 12 metals with benzopyridine- and benzopyrazine-type ligands or cations,<sup>2</sup> a variety of neutral tetrahedra and anionic tetrahalometallates were obtained in the current study, employing the organic ligands/cations quinolinium, acridine/acridinium and phenazine/phenazinium. The organic ligands investigated in this study differ from the organic pyridine-type ligands employed by Bowmaker,<sup>1</sup> in that the pyridine backbone is benzo-substituted, whereas the pyridine-type ligands used by Bowmaker<sup>1</sup> are methyl-substituted. The focus on benzo-substituted pyridine ligands/cations is motivated by the contribution that the structures make towards understanding the effect of increasing aromatic surface area of the ligand/cation on the structures obtained. None of the neutral compounds reported here resemble the  $\text{ML}_2\text{X}_2$  adducts reported by Bowmaker,<sup>1</sup> instead the benzopyridine- and benzopyrazine-type N-donor ligands are found to be uncoordinated neutral molecules, and the tetrahedral metal centre is, in addition to two halido ligands, further coordinated by either aqua or solvent ligands, instead of coordinating to the respective  $d^{10}$  metal cations, as was the case with Bowmaker's adducts. This observation is attributed to the steric effect of the size of the organic ligands employed.

## Results

The novel structures of sixteen zero-dimensional compounds were determined, and are presented in Table 1, together with the CSD reference codes of related structures available in the literature, as they appear in the CSD (version 5.35, May 2015 update).<sup>3</sup> The CSD search fragments comprised the inorganic  $ML_2X_2$  and  $[MX_4]^{2-}$  fragments with M, L and X in accordance with the column and row headings as set out in Table 1. In Table 1, L and L-H represent either the neutral or cationic organic unit as indicated by the column headings.  $M^{2+}$  indicates the divalent group 12 metal cation as specified, while X represents the respective halido ligand. Aqua ligands and isolated water molecules are represented by 'aq', with alcoholic solvent molecules or ligands indicated with 'sv'. Compounds **1** to **7** were prepared in the presence of an inorganic acid, HX, and as a result all represent anionic tetrahalometallates,  $[MX_4]^{2-}$ , with either  $Cd^{2+}$  or  $Hg^{2+}$  as the cationic metal center and quinolinium (quin-H), quinoxalium (quinox-H), acridinium (acr-H) or phenazinium (phe-H) as the counter cation. Compounds **8–16** contain  $Zn^{2+}$  as the tetrahedral cationic node. Five of the nine  $Zn^{2+}$  compounds are neutral, and four are ionic. Three of the four ionic  $Zn^{2+}$  compounds contain an anionic tetrahalometallate inorganic moiety,  $[ZnX_4]^{2-}$ , while the inorganic component of the fourth ionic  $Zn^{2+}$  compound is coordinated by three halido ligands and one aqua ligand,  $[ZnX_3(H_2O)]^-$ . Crystallographic data for all of the structures are listed in Table 2.

**Table 1** Novel structures determined in this study with allocated numbering scheme and the CSD reference codes of related compounds available in the literature

$M^{2+}$	X	acr		acr-H		phe		phe-H	
$Zn^{2+}$	$Cl^-$			$[L-H]_2[MX_4]$	<b>6</b>	$[L]_2[MX_2(aq)_2] \cdot H_2O$	<b>12</b>	$[L]_2[MX_4]$	<b>10</b>
	$Br^-$	$[L_3][MX_2(aq)_2]$	<b>14</b>	$[L-H]_2[MX_4]$	<b>7</b>	$[L]_2[MX_2(aq)_2] \cdot H_2O$	<b>13</b>	$[L-H][L][MX_3(aq)] \cdot H_2O \cdot sv$	<b>11</b>
	$I^-$	$[L_3][MX_2(aq)(sv)]$	<b>15</b> <b>16</b>						
$Cd^{2+}$	$Cl^-$			$[L-H]_2[MX_4]$	<b>8</b>				
	$Br^-$			$[L-H]_2[MX_4]$	<b>9</b>			$[L-H]_2[MX_4] \cdot 2(H_2O)$	<b>3</b>
	$I^-$								
$Hg^{2+}$	$Cl^-$							$[L-H]_2[MX_4] \cdot 2(H_2O)$	<b>1</b>
	$Br^-$							$[L-H]_2[MX_4] \cdot 2(H_2O)$	<b>2</b>
	$I^-$								

		quin	quin-H	quinox	quinox-H
$Zn^{2+}$	$Cl^-$	$ML_2X_2$ , PUVJIZ <sup>3,4</sup>	$[L-H][MLX_3]$ , CABQEC <sup>5</sup> $[L]_2[MX_4] \cdot H_2O$ , CASMOZ <sup>5,6</sup>	$ML_2X_2$ , PVVAWM01 <sup>7</sup>	
	$Br^-$	$ML_2X_2$ , EYETAIE <sup>1</sup>		$ML_2X_2$ , WIHKUU <sup>7</sup>	
	$I^-$	$ML_2X_2$ , KAKYIE <sup>1</sup>			
$Cd^{2+}$	$Cl^-$		$[L-H]_2[MX_4] \cdot H_2O$	<b>5</b>	
	$Br^-$				
	$I^-$				
$Hg^{2+}$	$Cl^-$				

		quin	quin-H		quinox	quinox-H
	Br <sup>-</sup>		[L-H] <sub>2</sub> [MX <sub>4</sub> ]aq	4		
	I <sup>-</sup>					
		pyr	pyr-H	pyz	pyz-H	
Zn <sup>2+</sup>	Cl <sup>-</sup>	ML <sub>2</sub> X <sub>2</sub> , ZNPYRC01 <sup>8</sup>	[L-H] <sub>2</sub> [MX <sub>4</sub> ], WOHFII <sup>9</sup>			
	Br <sup>-</sup>	ML <sub>2</sub> X <sub>2</sub> , GITCUH <sup>10</sup>				
	I <sup>-</sup>	ML <sub>2</sub> X <sub>2</sub> , ZNPYDI <sup>11</sup>				
Cd <sup>2+</sup>	Cl <sup>-</sup>					
	Br <sup>-</sup>		[L-H] <sub>2</sub> [MX <sub>4</sub> ]·H <sub>2</sub> O, FAXNAU <sup>12</sup>			
	I <sup>-</sup>	ML <sub>2</sub> X <sub>2</sub> , IPAYAZ <sup>13</sup>				
Hg <sup>2+</sup>	Cl <sup>-</sup>					
	Br <sup>-</sup>	ML <sub>2</sub> X <sub>2</sub> , BEJLAD <sup>14</sup>				
	I <sup>-</sup>	ML <sub>2</sub> X <sub>2</sub> , BEJLEH <sup>14</sup>				

**Table 2** Crystallographic parameters for compounds 1–16

Parameter	1	2	3
Abbreviation	[phe-H] <sub>2</sub> [HgCl <sub>4</sub> ]·2H <sub>2</sub> O	[phe-H] <sub>2</sub> [HgBr <sub>4</sub> ]·2H <sub>2</sub> O	[phe-H] <sub>2</sub> [CdBr <sub>4</sub> ]·2H <sub>2</sub> O
Empirical formula	C <sub>24</sub> H <sub>22</sub> N <sub>4</sub> O <sub>2</sub> HgCl <sub>4</sub>	C <sub>24</sub> H <sub>22</sub> N <sub>4</sub> O <sub>2</sub> HgBr <sub>4</sub>	C <sub>24</sub> H <sub>22</sub> N <sub>4</sub> O <sub>2</sub> CdBr <sub>4</sub>
M (g mol <sup>-1</sup> )	740.84	918.68	830.49
Temperature (K)	296(2)	293(2)	293(2)
Crystal system	Monoclinic	Monoclinic	Monoclinic
Space group	P2 <sub>1</sub> /c	P2 <sub>1</sub> /c	P2 <sub>1</sub> /c
a/Å	16.448(2)	16.5361(14)	16.6930(15)
b/Å	13.1972(14)	13.2372(11)	13.4439(12)
c/Å	12.5022(14)	12.7563(11)	12.7863(11)
α/°	90	90	90
β/°	106.338(4)	106.250(3)	106.754(2)
γ/°	90	90	90
Volume (Å <sup>3</sup> )	2604.2(5)	2680.7(4)	2747.7(4)
Z	4	4	4
Density (calculated) (Mg m <sup>-3</sup> )	1.890	2.276	2.008
Absorption coefficient (mm <sup>-1</sup> )	6.351	11.733	6.640
F(000)	1432	1720	1592
Theta range for data collection (°)	2.294 to 26.372	2.266 to 26.368	2.250 to 26.371
Reflections collected	14 134	41 629	195 792
Independent reflections	5317 [R <sub>(int)</sub> = 0.0520]	5375 [R <sub>(int)</sub> = 0.1276]	5605 [R <sub>(int)</sub> = 0.1749]
Completeness to θ = 25° (%)	99.8	99.1	100.0

Parameter	1	2	3
Max. and min. transmission	0.7457 and 0.5166	0.7457 and 0.1814	0.7454 and 0.4797
Data/restraints/parameters	5317/6/334	5375/0/166	5605/2/319
Goodness-of-fit on $F^2$	1.002	1.175	1.126
Final R indices [ $I > 2\sigma(I)$ ]	$R_1 = 0.0447$ , $wR_2 = 0.0586$	$R_1 = 0.1115$ , $wR_2 = 0.1800$	$R_1 = 0.0755$ , $wR_2 = 0.1331$
R indices (all data)	$R_1 = 0.0990$ , $wR_2 = 0.0685$	$R_1 = 0.1426$ , $wR_2 = 0.1901$	$R_1 = 0.1288$ , $wR_2 = 0.1569$
Largest diff. peak and hole ( $e \text{ \AA}^{-3}$ )	0.806 and $-0.960$	3.911 and $-2.464$	4.241 and $-2.128$

Parameter	4	5	6
Abbreviation	[quin-H] <sub>2</sub> [CdBr <sub>4</sub> ]-H <sub>2</sub> O	[quin-H] <sub>2</sub> [HgCl <sub>4</sub> ]-H <sub>2</sub> O	[acr-H] <sub>2</sub> [ZnCl <sub>4</sub> ]
Empirical formula	C <sub>18</sub> H <sub>20</sub> N <sub>2</sub> O <sub>2</sub> CdBr <sub>4</sub>	C <sub>18</sub> H <sub>20</sub> N <sub>2</sub> O <sub>2</sub> HgCl <sub>4</sub>	C <sub>26</sub> H <sub>20</sub> N <sub>2</sub> ZnCl <sub>4</sub>
M ( $\text{g mol}^{-1}$ )	728.40	638.75	567.61
Temperature (K)	296(2)	293(2)	293(2)
Crystal system	Monoclinic	Monoclinic	Monoclinic
Space group	C2/c	C2/c	C2/c
a/ $\text{\AA}$	12.5712(12)	12.0377(9)	13.155(13)
b/ $\text{\AA}$	10.2622(9)	9.9002(7)	10.375(11)
c/ $\text{\AA}$	18.6905(18)	18.3254(13)	18.777(17)
$\alpha$ / $^\circ$	90	90	90
$\beta$ / $^\circ$	101.379(3)	100.720(2)	93.87(3)
$\gamma$ / $^\circ$	90	90	90
Volume ( $\text{\AA}^3$ )	2363.8(4)	2145.8(3)	2557(4)
Z	4	4	4
Density (calculated) ( $\text{Mg m}^{-3}$ )	2.047	1.977	1.475
Absorption coefficient ( $\text{mm}^{-1}$ )	7.700	7.687	1.396
F(000)	1384	1224	1152
Theta range for data collection ( $^\circ$ )	2.223 to 26.368	2.262 to 26.360	2.502 to 25.680
Reflections collected	10 002	40 959	19 674
Independent reflections	2411 [ $R_{\text{int}} = 0.0493$ ]	2196 [ $R_{\text{int}} = 0.0348$ ]	2389 [ $R_{\text{int}} = 0.1168$ ]
Completeness to $\theta = 25^\circ$ (%)	99.7	99.9	98.0
Max. and min. transmission	0.7462 and 0.4828	0.7479 and 0.5244	0.7460 and 0.5649
Data/restraints/parameters	2411/3/135	2196/1/135	2389/0/150
Goodness-of-fit on $F^2$	1.002	1.094	1.185
Final R indices [ $I > 2\sigma(I)$ ]	$R_1 = 0.0374$ , $wR_2 = 0.0720$	$R_1 = 0.0119$ , $wR_2 = 0.0292$	$R_1 = 0.1423$ , $wR_2 = 0.2463$
R indices (all data)	$R_1 = 0.0692$ , $wR_2 = 0.0806$	$R_1 = 0.0127$ , $wR_2 = 0.0295$	$R_1 = 0.2053$ , $wR_2 = 0.2719$
Largest diff. peak and hole ( $e \text{ \AA}^{-3}$ )	1.049 and $-0.592$	0.676 and $-0.239$	0.729 and $-0.696$

Parameter	7	8	9
Abbreviation	[acr-H] <sub>2</sub> [ZnBr <sub>4</sub> ]	[acr-H] <sub>2</sub> [CdCl <sub>4</sub> ]	[acr-H] <sub>2</sub> [CdBr <sub>4</sub> ]
Empirical formula	C <sub>26</sub> H <sub>20</sub> N <sub>2</sub> ZnBr <sub>4</sub>	C <sub>26</sub> H <sub>20</sub> N <sub>2</sub> CdCl <sub>4</sub>	C <sub>26</sub> H <sub>20</sub> N <sub>2</sub> CdBr <sub>4</sub>
M (g mol <sup>-1</sup> )	745.45	614.64	792.48
Temperature (K)	293(2)	293(2)	293(2)
Crystal system	Monoclinic	Monoclinic	Triclinic
Space group	C2/c	C2/c	P $\bar{1}$
a/Å	13.1044(13)	12.8432(16)	9.6262(4)
b/Å	10.2306(9)	10.2106(12)	10.2001(5)
c/Å	19.0699(19)	18.821(2)	14.7243(7)
$\alpha$ /°	90	90	97.3750(10)
$\beta$ /°	92.513(3)	92.326(5)	93.4720(10)
$\gamma$ /°	90	90	113.2140(10)
Volume (Å <sup>3</sup> )	2554.2(4)	2466.1(5)	1307.87(10)
Z	4	4	2
Density (calculated) (Mg m <sup>-3</sup> )	1.939	1.655	2.012
Absorption coefficient (mm <sup>-1</sup> )	7.237	1.337	6.963
F(000)	1440	1224	756
Crystal size (mm <sup>3</sup> )	0.249 × 0.174 × 0.050	0.278 × 0.262 × 0.048	0.160 × 0.160 × 0.100
Theta range for data collection (°)	2.527 to 28.009	2.166 to 26.371	2.203 to 26.372
Reflections collected	38 980	43 847	44 865
Independent reflections	3064 [R <sub>(int)</sub> = 0.0663]	2548 [R <sub>(int)</sub> = 0.0486]	5346 [R <sub>(int)</sub> = 0.0358]
Completeness to $\theta = 25^\circ$ (%)	100.0	100.0	100.0
Max. and min. transmission	0.7456 and 0.4813	0.7475 and 0.6609	0.7463 and 0.6066
Data/restraints/parameters	3064/0/151	2548/0/151	5346/2/306
Goodness-of-fit on F <sup>2</sup>	1.218	1.212	1.031
Final R indices [I > 2 $\sigma$ (I)]	R <sub>1</sub> = 0.0885, wR <sub>2</sub> = 0.2868	R <sub>1</sub> = 0.0765, wR <sub>2</sub> = 0.2109	R <sub>1</sub> = 0.0293, wR <sub>2</sub> = 0.0617
R indices (all data)	R <sub>1</sub> = 0.0986, wR <sub>2</sub> = 0.2974	R <sub>1</sub> = 0.0781, wR <sub>2</sub> = 0.2121	R <sub>1</sub> = 0.0435, wR <sub>2</sub> = 0.0667
Largest diff. peak and hole (e Å <sup>-3</sup> )	4.368 and -2.217	4.420 and -1.331	1.212 and -0.772

Parameter	10	11	12
Abbreviation	[phe-H <sub>2</sub> ]phe[ZnCl <sub>4</sub> ]	[phe-H](phe) <sub>2</sub> [Zn(OH <sub>2</sub> )Br <sub>3</sub> ]·EtOH·H <sub>2</sub> O	(phe) <sub>2</sub> [Zn(OH <sub>2</sub> ) <sub>2</sub> Cl <sub>2</sub> ]·H <sub>2</sub> O
Empirical formula	C <sub>36</sub> H <sub>28</sub> N <sub>6</sub> ZnCl <sub>4</sub>	C <sub>26</sub> H <sub>27</sub> N <sub>4</sub> O <sub>3</sub> ZnBr <sub>3</sub>	C <sub>24</sub> H <sub>22</sub> N <sub>4</sub> O <sub>3</sub> ZnCl <sub>2</sub>
M (g mol <sup>-1</sup> )	751.81	748.61	550.72
Temperature (K)	293(2)	293(2)	180(2)
Crystal system	Monoclinic	Triclinic	Monoclinic
Space group	C2/c	P $\bar{1}$	P2 <sub>1</sub> /c
a/Å	16.2283(14)	7.7519(3)	6.94010(10)
b/Å	12.5193(11)	10.0771(4)	16.5048(3)
c/Å	17.939(2)	18.7817(7)	20.9602(4)

Parameter	10	11	12
$\alpha/^\circ$	90	93.9740(10)	90
$\beta/^\circ$	115.769(2)	99.5510(10)	91.82(3)
$\gamma/^\circ$	90	104.5440(10)	90
Volume ( $\text{\AA}^3$ )	3282.2(6)	1390.97(9)	2399.67(8)
Z	4	2	4
Density (calculated) ( $\text{Mg m}^{-3}$ )	1.521	1.787	1.524
Absorption coefficient ( $\text{mm}^{-1}$ )	1.112	5.227	1.280
F(000)	1536	740	1128
Crystal size ( $\text{mm}^3$ )	$0.379 \times 0.156 \times 0.108$	$0.239 \times 0.167 \times 0.116$	$0.180 \times 0.180 \times 0.050$
Theta range for data collection ( $^\circ$ )	2.521 to 26.372	2.259 to 26.371	2.303 to 26.372
Reflections collected	52 068	62 920	31 320
Independent reflections	3370 [ $R_{\text{int}} = 0.1273$ ]	5694 [ $R_{\text{int}} = 0.1050$ ]	4937 [ $R_{\text{int}} = 0.0898$ ]
Completeness to $\theta = 25^\circ$ (%)	99.9	99.8	100.0
Max. and min. transmission	0.7457 and 0.6316	0.7456 and 0.5722	0.886 and 0.775
Data/restraints/parameters	3370/2/221	5694/6/358	4937/6/332
Goodness-of-fit on $F^2$	1.115	1.050	1.141
Final R indices [ $I > 2\sigma(I)$ ]	$R_1 = 0.0567$ , $wR_2 = 0.1321$	$R_1 = 0.0237$ , $wR_2 = 0.0624$	$R_1 = 0.1013$ , $wR_2 = 0.3008$
R indices (all data)	$R_1 = 0.0689$ , $wR_2 = 0.1394$	$R_1 = 0.0258$ , $wR_2 = 0.0634$	$R_1 = 0.1208$ , $wR_2 = 0.3213$
Largest diff. peak and hole ( $e \text{\AA}^{-3}$ )	1.043 and $-0.636$	0.744 and $-0.503$	3.150 and $-1.038$

Parameter	13	14	15
Abbreviation	(phe) <sub>2</sub> [Zn(OH <sub>2</sub> ) <sub>2</sub> Br <sub>2</sub> ]·H <sub>2</sub> O	(acr) <sub>3</sub> [Zn(OH <sub>2</sub> ) <sub>2</sub> Br <sub>2</sub> ]	(acr) <sub>3</sub> [Zn(OH <sub>2</sub> )I <sub>2</sub> (O-prop)]
Empirical formula	C <sub>24</sub> H <sub>22</sub> N <sub>4</sub> O <sub>3</sub> ZnBr <sub>2</sub>	C <sub>39</sub> H <sub>31</sub> N <sub>3</sub> O <sub>2</sub> ZnBr <sub>2</sub>	C <sub>42</sub> H <sub>37</sub> N <sub>3</sub> O <sub>2</sub> ZnI <sub>2</sub>
M ( $\text{g mol}^{-1}$ )	639.64	798.86	934.91
Temperature (K)	293(2)	100(2)	293(2)
Crystal system	Monoclinic	Monoclinic	Monoclinic
Space group	P2 <sub>1</sub> /c	P2 <sub>1</sub> /n	P2 <sub>1</sub> /n
a/ $\text{\AA}$	6.9170(7)	10.788(2)	11.4956(3)
b/ $\text{\AA}$	16.4068(15)	20.604(5)	21.8349(7)
c/ $\text{\AA}$	21.562(2)	15.212(3)	15.5772(5)
$\alpha/^\circ$	90	90	90
$\beta/^\circ$	92.213(2)	96.743(3)	93.7720(10)
$\gamma/^\circ$	90	90	90
Volume ( $\text{\AA}^3$ )	2445.2(4)	3358.1(13)	3901.5(2)
Z	4	4	4

Parameter	13	14	15
Density (calculated) (Mg m <sup>-3</sup> )	1.738	1.580	1.592
Absorption coefficient (mm <sup>-1</sup> )	4.307	3.151	2.250
F(000)	1272	1608	1848
Theta range for data collection (°)	2.262 to 26.370	1.671 to 26.372	2.275 to 26.372
Reflections collected	108 310	18 892	96 261
Independent reflections	5010 [R <sub>(int)</sub> = 0.0695]	6812 [R <sub>(int)</sub> = 0.0743]	7976 [R <sub>(int)</sub> = 0.0343]
Completeness to $\theta = 25^\circ$ (%)	99.9	99.5	99.9
Max. and min. transmission	0.7485 and 0.4721	0.7450 and 0.4356	0.7454 and 0.5554
Data/restraints/parameters	5010/0/332	6812/8/440	7976/3/465
Goodness-of-fit on F <sup>2</sup>	1.065	0.993	1.023
Final R indices [I > 2 $\sigma$ (I)]	R <sub>1</sub> = 0.0473, wR <sub>2</sub> = 0.1189	R <sub>1</sub> = 0.0391, wR <sub>2</sub> = 0.0954	R <sub>1</sub> = 0.0364, wR <sub>2</sub> = 0.0847
R indices (all data)	R <sub>1</sub> = 0.0551, wR <sub>2</sub> = 0.1246	R <sub>1</sub> = 0.0564, wR <sub>2</sub> = 0.0996	R <sub>1</sub> = 0.0548, wR <sub>2</sub> = 0.0951
Largest diff. peak and hole (e Å <sup>-3</sup> )	1.307 and -0.909	0.661 and -0.469	1.572 and -1.127

Parameter	16
Abbreviation	(acr) <sub>3</sub> [Zn(OH <sub>2</sub> )I <sub>2</sub> (O-EtOH)]
Empirical formula	C <sub>41</sub> H <sub>35</sub> N <sub>3</sub> O <sub>2</sub> ZnI <sub>2</sub>
M (g mol <sup>-1</sup> )	920.89
Temperature (K)	120(2)
Crystal system	Monoclinic
Space group	P2 <sub>1</sub> /n
a/Å	11.2134(5)
b/Å	21.5564(11)
c/Å	15.1841(8)
$\alpha$ /°	90
$\beta$ /°	92.675(2)
$\gamma$ /°	90
Volume (Å <sup>3</sup> )	3666.3(3)
Z	4
Density (calculated) (Mg m <sup>-3</sup> )	1.668
Absorption coefficient (mm <sup>-1</sup> )	2.393
F(000)	1816
Theta range for data collection (°)	1.889 to 26.370
Reflections collected	113 425
Independent reflections	7469 [R <sub>(int)</sub> = 0.0510]
Completeness to $\theta = 25^\circ$ (%)	99.8
Max. and min. transmission	0.7481 and 0.544
Data/restraints/parameters	7469/3/455
Goodness-of-fit on F <sup>2</sup>	0.824

Parameter	16
Final R indices [ $I > 2\sigma(I)$ ]	$R_1 = 0.0211$ , $wR_2 = 0.0591$
R indices (all data)	$R_1 = 0.0231$ , $wR_2 = 0.0617$
Largest diff. peak and hole ( $e \text{ \AA}^{-3}$ )	1.037 and $-0.335$

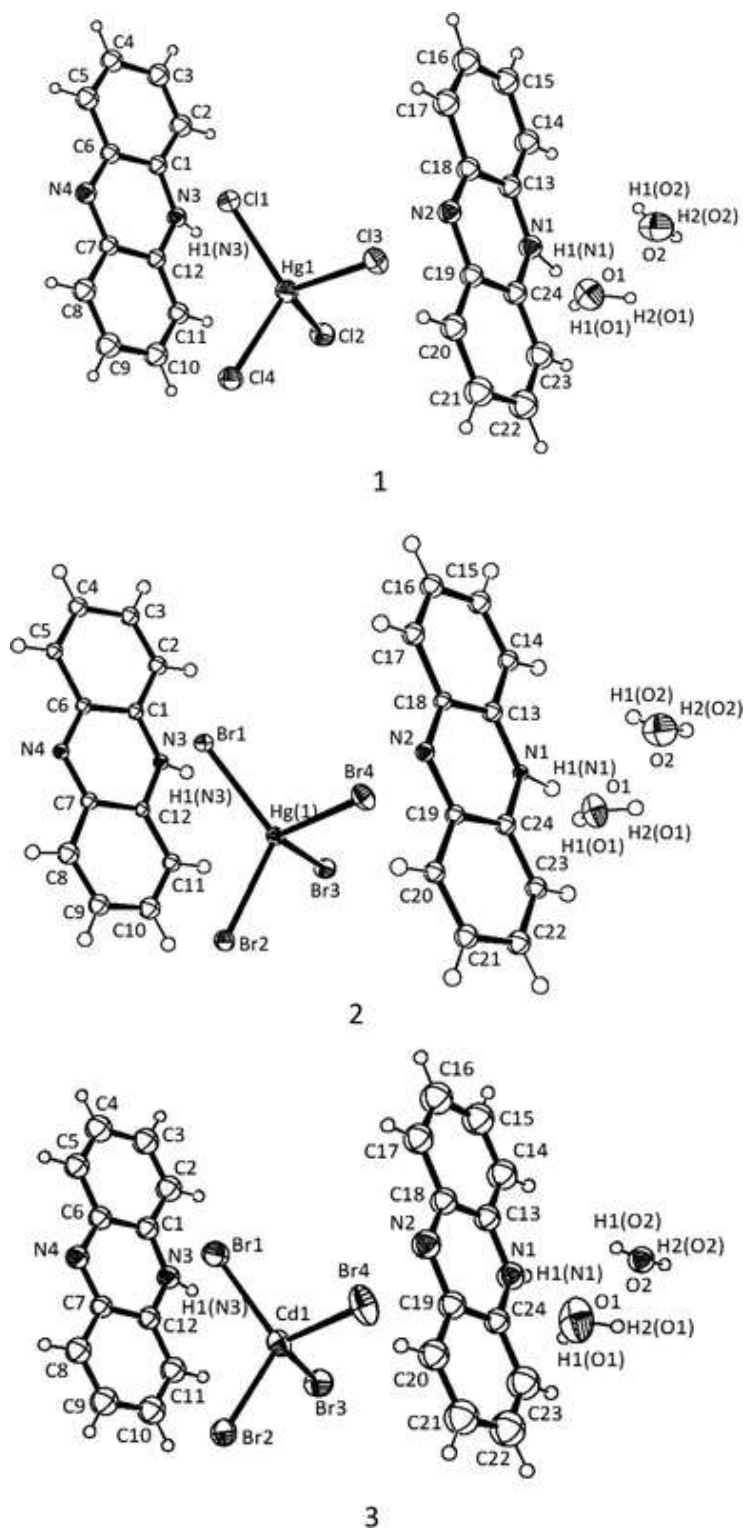


**Fig. 1** Asymmetric units of **1–3**, showing the atomic numbering scheme. Displacement ellipsoids are shown at the 50% probability level and hydrogen atoms are shown as small spheres of arbitrary radii.



## [phe-H]<sub>2</sub>[HgCl<sub>4</sub>]·2H<sub>2</sub>O (**1**), [phe-H]<sub>2</sub>[HgBr<sub>4</sub>]·2H<sub>2</sub>O (**2**) and [phe-H]<sub>2</sub>[CdBr<sub>4</sub>]·2H<sub>2</sub>O (**3**)

The asymmetric units of **1** and **2** consist of a Hg<sup>2+</sup> cation coordinated to four halido ligands, two isolated, crystallographically independent phenazinium ligands, denoted as A and B (for those containing atoms N1 and N3, respectively), and two isolated water molecules, as illustrated in Fig. 1. Compound **3** differs from compounds **1** and **2** in that the metal centre comprises a four-coordinate Cd<sup>2+</sup> cation. The compounds crystallise in the monoclinic space group P2<sub>1</sub>/c and are isostructural.

The Hg<sup>2+</sup> ion is coordinated by four halido ligands, in a tetrahedral fashion, with ∠(XHgX)s ranging between 104.19(5)° and 115.09(5)° for **1** and 103.34(7)° and 116.08(7)° for **2**. Hg–X bond distances range between 2.445(2) Å and 2.516(2) Å for **1** and 2.571(2) Å and 2.624(2) Å for **2**. The local coordination sphere of the Cd<sup>2+</sup> metal centre in **3** also has its tetrahedral coordination geometry completed by four coordinated halido ligands, with the smallest ∠(XCdX) being 104.22(5)° and the largest being 113.93(5)°, with X = Br. The Cd–Br bond distances in **3** vary between 2.574(1) Å and 2.615(1) Å. In compounds **1** and **2**, the largest Hg–X distance corresponds to the bond which contains the X(2) ligand. This is due to the strong hydrogen bond, N(3)–H1···X(2)–Hg(1), that connects the phenazinium ligand B to the tetrahalometallate moieties of both **1** and **2**. Hydrogen bonding interactions are listed in Table 9. Within the asymmetric unit, the O(2)-containing water molecule further connects the tetrahalometallate moiety by forming a hydrogen bond to the X(3) halido ligand. The two water molecules are connected by an O(1)–H2···O(2) hydrogen bond, with the phenazinium ligand B in turn connected to the O(1)-containing water molecule via a N(1)–H1···O(1) hydrogen bond.

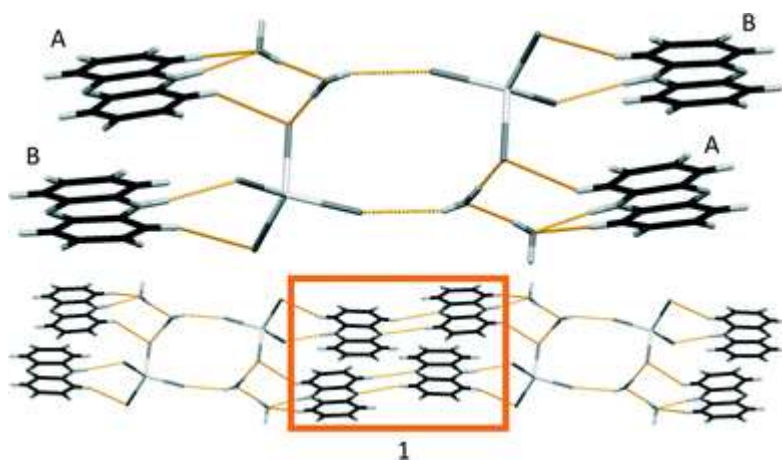
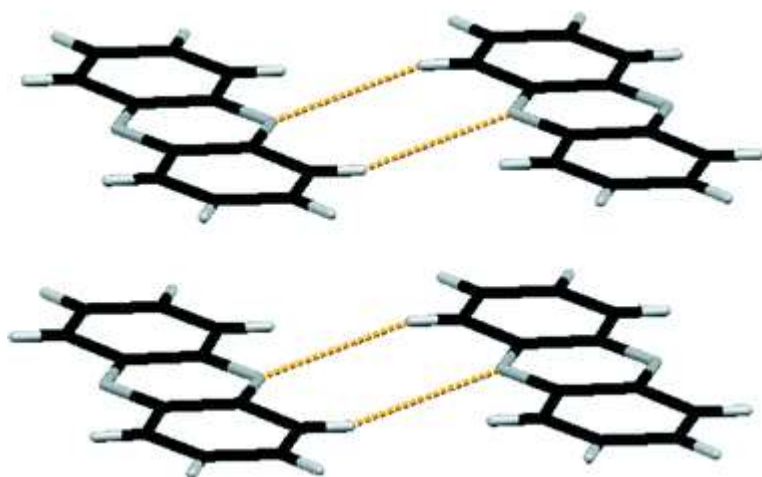
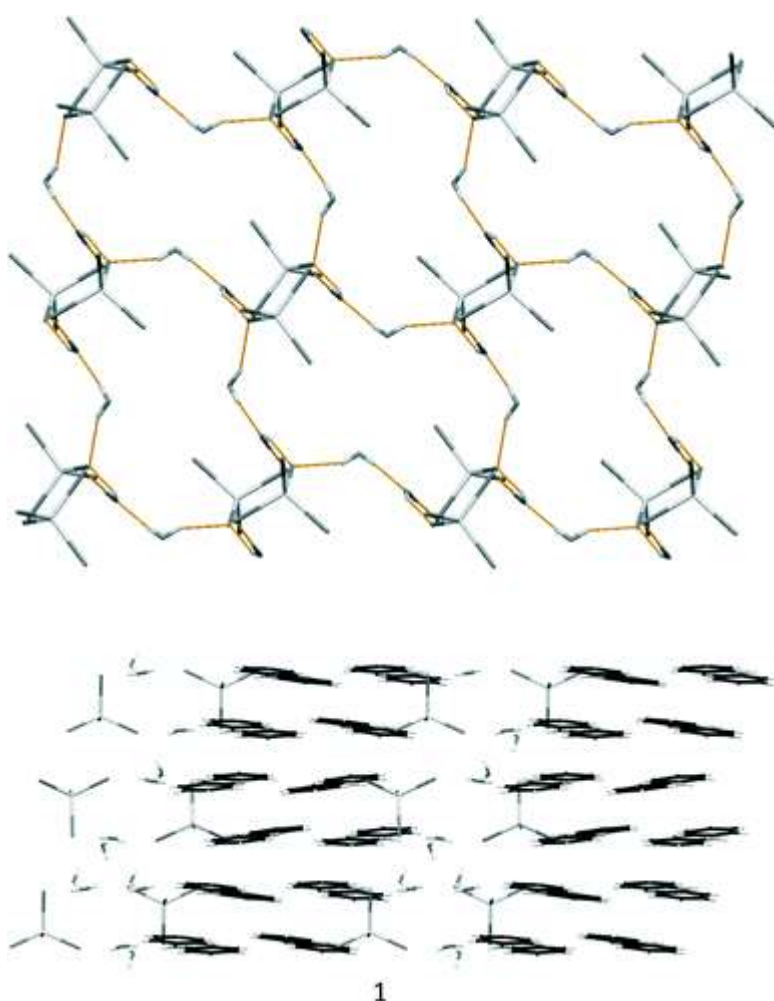


Fig. 2 Hydrogen-bonded aggregate along the bc-plane (top). Weak hydrogen bonding contacts between phenazinium ligands along the bc-plane of **1** (bottom).

Expansion of the hydrogen bond contacts along the bc-plane produces the hydrogen-bonded aggregate illustrated in Fig. 2(top). The decameric hydrogen-bonded aggregate is related by an inversion centre at [0, 0, 0]. Strong hydrogen bonding along the diagonal direction of the bc-plane terminates upon formation of the said aggregate. Weak tail-to-tail hydrogen bonding interactions, C(17)–H(17)···N(2) and C(5)–H(5)···N(4), between the phenazinium ligands further connect adjacent decameric hydrogen-bonded aggregates, as illustrated in Fig. 2(bottom). This motif has survived as remnants of the  $\alpha$ -polymorph of phenazine, PHENAZ04,<sup>15</sup> which was used as the starting material in the synthesis of compound **1**, the motif of which is illustrated in Fig. 3.



**Fig. 3** Weak hydrogen-bonded motif observed in the  $\alpha$ -polymorph of phenazine, PHENAZ04.<sup>15</sup>



**Fig. 4** Jagged brick paving pattern of the two-dimensional hydrogen-bonded sheet formed by the inorganic component of compound **1** when viewed down the crystallographic  $a$ -axis (top). Inorganic and organic double layers as viewed down the reciprocal  $c^*$ -lattice (bottom).

The inorganic components of compounds **1–3** form two-dimensional hydrogen-bonded sheets parallel to the  $bc$ -plane which, when viewed perpendicular to the crystallographic  $a$ -axis, can be likened to jagged brick paving, as illustrated in Fig. 4(top). Strong, charge-assisted  $N(1)-H1 \cdots O(1)$  and  $N(3)-H1 \cdots X(2)$  hydrogen bonds further connect the phenazinium cations to

the jagged brick sheet described above. Weak tail-to-tail hydrogen bonding interactions between phenazinium moieties extend the network by connecting adjacent decameric hydrogen-bonded aggregates, as shown in Fig. 2.

This means that the weak hydrogen bond donors and acceptors are hydrogen-bonded to each other while the strong donors and acceptors interact, as predicted by Etter.<sup>16</sup> In compounds **1**–**3**, the molecules and ions pack in alternating inorganic and organic double layers, as illustrated in Fig. 4(bottom).

The centroid-to-centroid distances between the nitrogen-containing six-membered rings of the phenazinium cations range between 3.950(3) Å and 3.964(6) Å for compounds **1** and **3**. As reflected by the non-zero  $\alpha$  angle, the interacting rings are not parallel. The ring interaction parameters of compounds **1** and **2**, as defined in PLATON,<sup>17</sup> are listed in Table 10, with  $d(\text{Cg}-\text{Cg}) < 6.0$  Å and  $\beta < 60^\circ$ . In addition to the described hydrogen bonding and aromatic interactions, further non-covalent anion–aromatic interactions between the aromatic moieties and the X(1) and X(4) halido ligands of the respective tetrahalometallates are present, as illustrated in Fig. 5. All anion–aromatic interactions, as defined in PLATON,<sup>17</sup> are collated in Table 11.

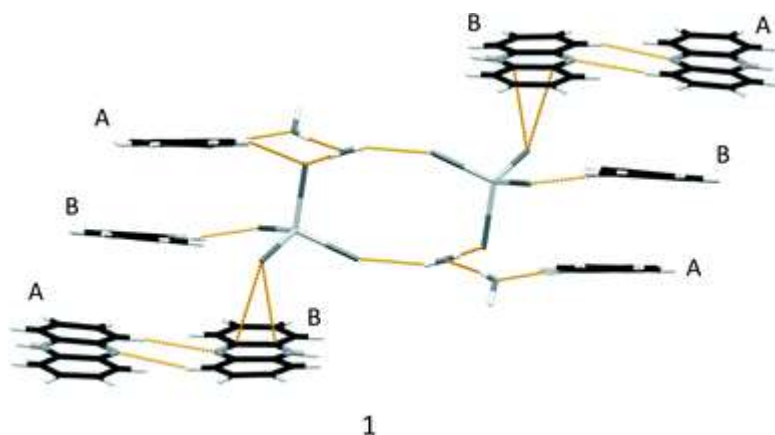
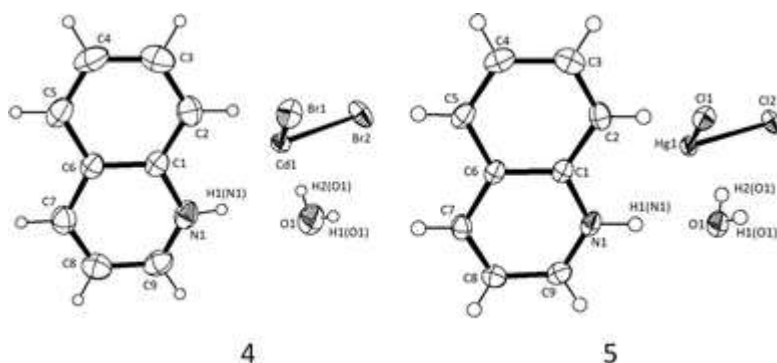


Fig. 5 Anion–aromatic interactions present in compound **1**.

#### [quin-H]<sub>2</sub>[CdBr<sub>4</sub>]·H<sub>2</sub>O (**4**) and [quin-H]<sub>2</sub>[HgCl<sub>4</sub>]·H<sub>2</sub>O (**5**)

Ionic compounds **4** and **5** are isostructural. The asymmetric units of **4** and **5** consist of a Cd<sup>2+</sup> ion and a Hg<sup>2+</sup> ion, respectively, coordinated to two halido ligands with one isolated water molecule each, as illustrated in Fig. 6. The compounds differ further still in that the coordinated bromido ligands in **4** are isomorphously replaced with chlorido ligands in compound **5**. The compounds crystallise in the monoclinic space group C2/c. Their crystallographic parameters are listed in Table 1.



**Fig. 6** Asymmetric units of **4** and **5**, showing the atomic numbering scheme. Displacement ellipsoids are shown at the 30% probability level for **4** and at the 50% probability level for **5** with hydrogen atoms shown as small spheres of arbitrary radii.

The complete tetrahedral unit in both compounds is generated by a 2-fold rotation axis along  $[0, 1, 0]$ , as illustrated in Fig. 7. The local tetrahedral  $M^{2+}$  coordination sphere in both compounds comprises four halido ligands with  $\angle(X-M-X)$ s ranging between  $105.704(19)^\circ$  and  $112.61(4)^\circ$  for **4** and  $103.069(14)^\circ$  and  $110.890(14)^\circ$  for **5**.  $M-X$  bond distances range between  $2.5500(6)$  Å and  $2.5872(6)$  Å for **4** and  $2.4348(4)$  Å and  $2.5163(4)$  Å for **5**, as collated in Table 3. The shorter bond distances in both compounds belong to  $M-X$  bonds acting as hydrogen bond acceptors from two different water molecules. In compound **4**, strong  $O(1)-H(1O1)\cdots Br(1)$  and  $O(1)-H(2O1)\cdots Br(1)$  hydrogen bonds between the hydrogen atoms of the water molecules and the tetrahalometallate moiety, with  $D-H\cdots A$  distances of  $2.95(9)$  Å and  $2.60(11)$  Å, respectively, connect the inorganic units into a two-dimensional sheet along the  $ab$ -plane, as illustrated in Fig. 8(top) and listed in Table 9.

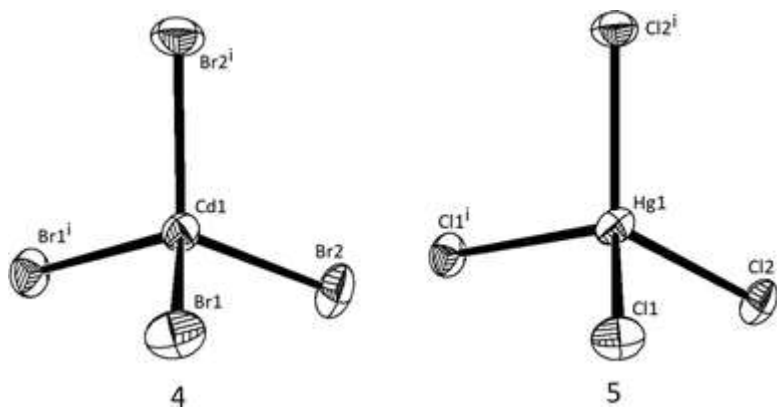


**Fig. 7** Inorganic anionic tetrahedral units in **4** and **5** generated by a 2-fold rotation axis along the  $[0, 1, 0]$  direction, showing the atomic numbering scheme of symmetry-generated halido ligands. Displacement ellipsoids are shown at the 30% probability level for **4** and at the 50% probability level for **5**. Symmetry operator used to generate equivalent atoms:  $^i -x, y, 1/2 - z$ .

**Table 3** Selected M–X bond lengths and X–M–X angles in **4** and **5** (Å, °), with M = Cd (**4**), Hg (**5**) and X = Br (**4**), Cl (**5**)

	<b>4</b>	<b>5</b>	Symmetry operator
M(1)–X(2) <sup>#1</sup>	2.5501(6)	2.4348(4)	#1 –x, y, –z + 1/2
M(1)–X(2)	2.5500(6)	2.4348(4)	
M(1)–X(1) <sup>#1</sup>	2.5872(6)	2.5162(4)	
M(1)–X(1)	2.5872(6)	2.5163(4)	
X(2) <sup>#1</sup> –M(1)–X(2)	112.61(4)	118.41(2)	
X(2) <sup>#1</sup> –M(1)–X(1) <sup>#1</sup>	105.704(19)	103.069(14)	
X(2)–M(1)–X(1) <sup>#1</sup>	111.07(2)	110.889(14)	
X(2) <sup>#1</sup> –M(1)–X(1)	111.07(2)	110.890(14)	
X(2)–M(1)–X(1)	105.705(18)	103.070(14)	
X(1) <sup>#1</sup> –M(1)–X(1)	110.78(3)	110.63(2)	

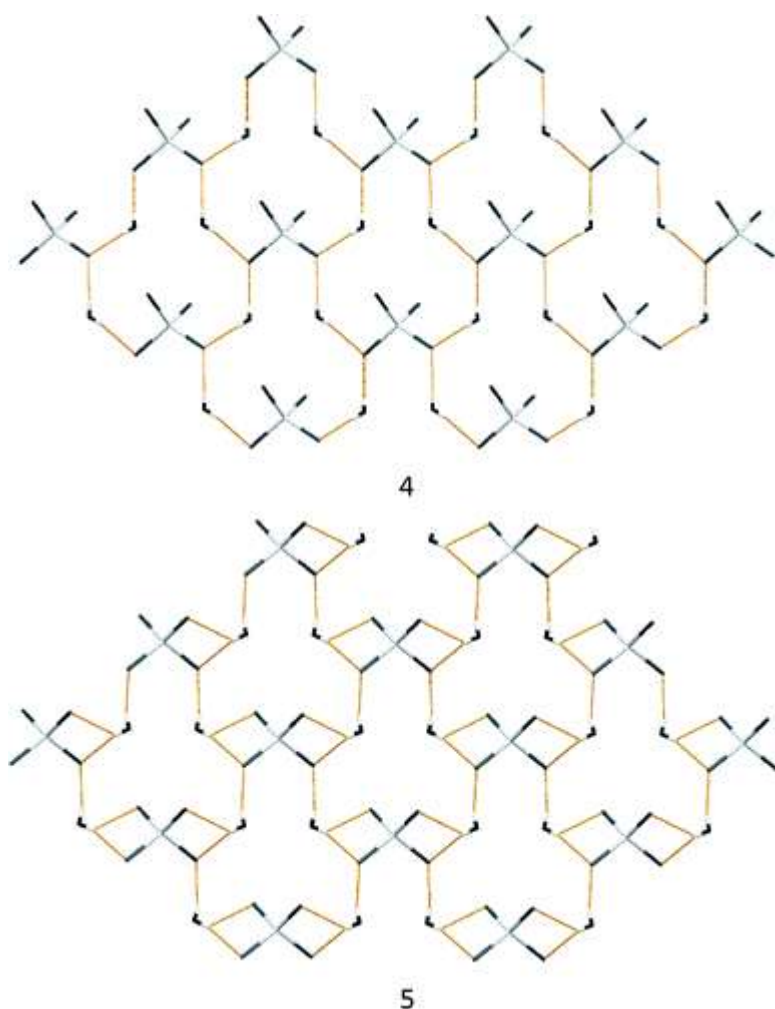


**Fig. 8** Hydrogen-bonded sheets observed in compounds **4** and **5**.

Remnants of the repeat-pear motif seen in **4** are still present in **5**, as shown in Fig. 8(bottom), where strong O(1)–H(1O1)···Cl(1) and bifurcated O(1)–H(2O1)···Cl(1) and O(1)–H(2O1)···Cl(2) hydrogen bonds between the hydrogen atoms of the water molecules and the

chlorido ligands of the tetrahedral units connect the inorganic units into a two-dimensional hydrogen-bonded sheet.

All four halido ligands in **5** engage as hydrogen bond-accepting atoms, whereas only two halido ligands have the same role in **4**. This is reflected in the tetrahedral geometry of the two systems, where the two small bond angles of  $103.069(14)^\circ$  in **5** lie between the chlorido atoms involved in bifurcation, causing a greater variation in internal tetrahedral bond angles than that observed in **4**, thus allowing the formation of additional hydrogen bonds.

The two-dimensional hydrogen-bonded sheet in **4** has quinolinium cations hydrogen-bonded to it through strong charge-assisted  $N(1)-H(1N1)\cdots O(1)$  hydrogen bonds to the oxygen atoms of the water molecules, with a  $d(D\cdots A)$  distance of  $2.779(6)$  Å, as illustrated in Fig. 9(top) and listed in Table 9.

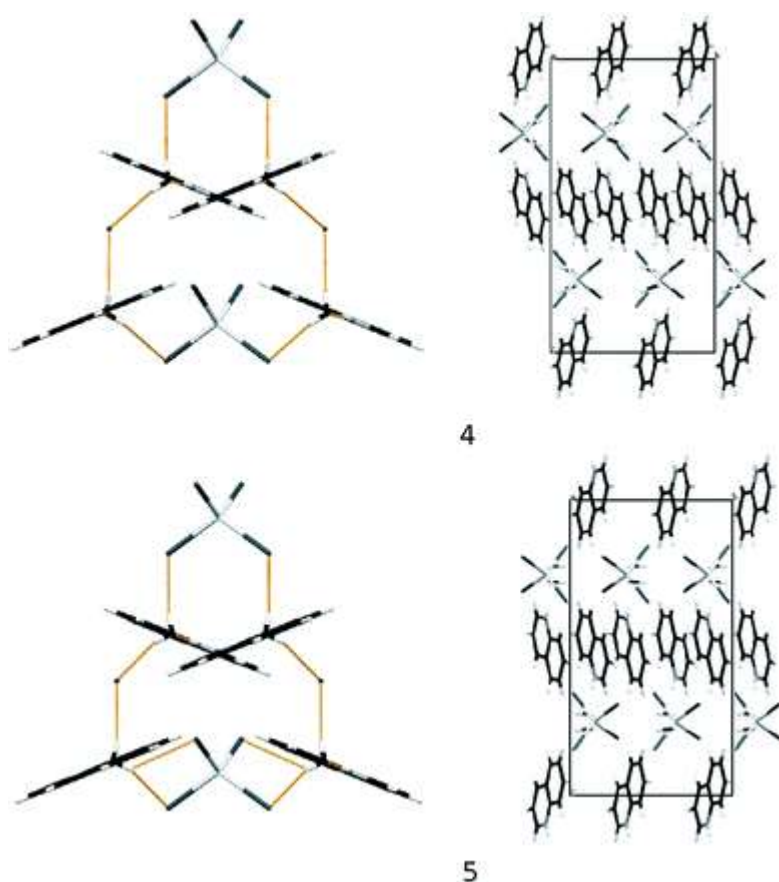


**Fig. 9** Attachment of quinolinium cations into the two-dimensional inorganic hydrogen-bonded sheet as viewed along the crystallographic *c*-axis (left) for both **4** and **5**. Interdigitation of quinolinium cations from adjacent two-dimensional sheets for both compounds (right) as viewed along the crystallographic *a*-axis.

The two-dimensional sheets further interact via non-covalent aromatic interactions by interdigitation of the planar quinolinium moieties that zip adjacent sheets together. The aromatic moieties are therefore slipped in a parallel manner with the nitrogen atoms in adjacent rings related by inversion. The centroid-to-centroid distance within the molecular zipper is  $3.943(3)$  Å, with a perpendicular slippage distance of  $1.733$  Å. Exactly the same pattern regarding hydrogen bonding from the quinolinium cations together with molecular zipping is observed for **5**, as illustrated in Fig. 9(bottom). The strong charge-assisted  $N(1)-H(1N1)\cdots O(1)$  hydrogen bonds are however slightly shorter with a  $d(D\cdots A)$  distance of



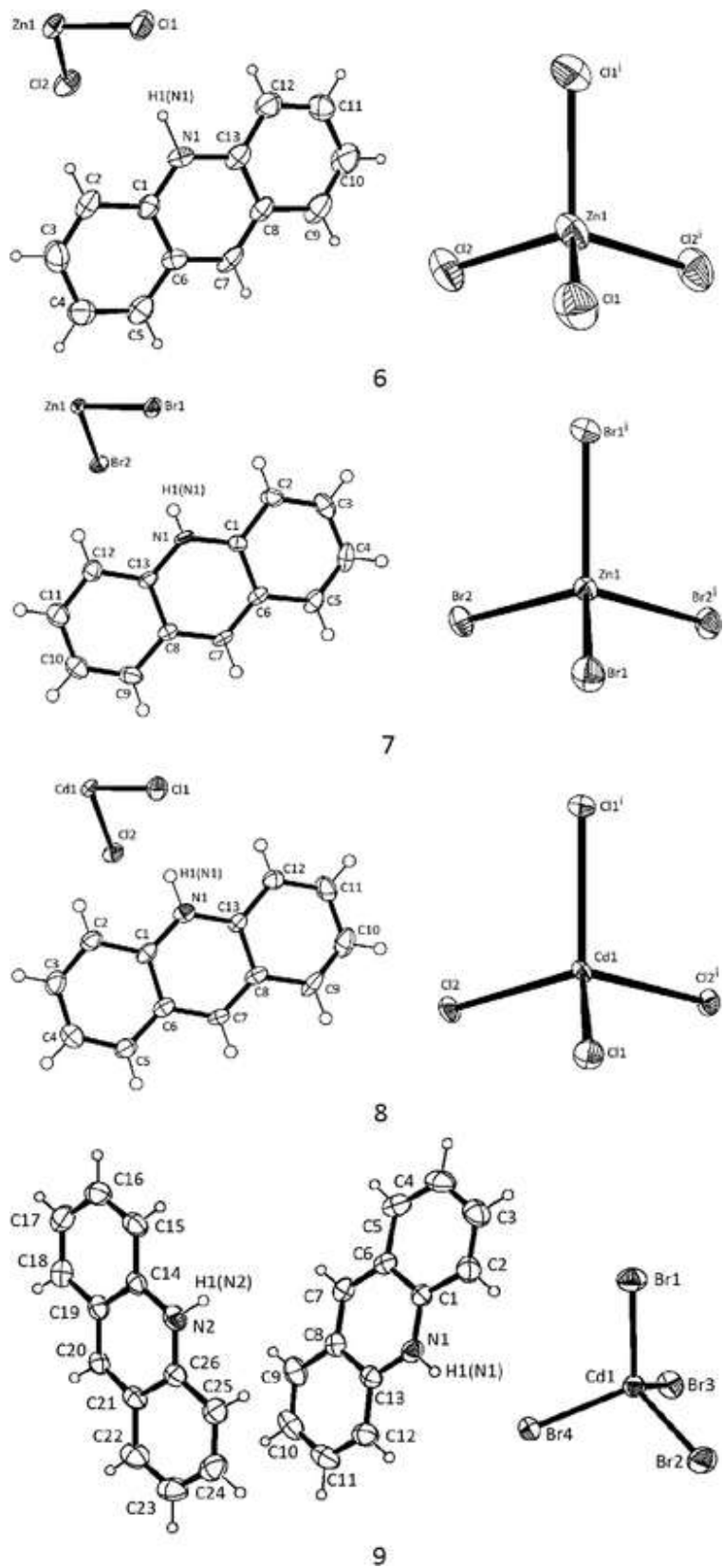


**Fig. 10** Asymmetric units of **6–9**, showing the atomic numbering scheme (left). The complete inorganic tetrahedral units in compounds **6–8** are indicated on the right hand side of the respective asymmetric units. Displacement ellipsoids are shown at the 50% probability level and hydrogen atoms are shown as small spheres of arbitrary radii. Symmetry operator used to generate equivalent atoms:  $i - x, y, 3/2 - z$ .

2.7375(18) Å, as well as shorter centroid-to-centroid and perpendicular slippage distances, which are now 3.8115(9) Å and 1.647 Å, respectively. The packing arrangement of compounds **4** and **5** can therefore be seen to be layered when viewed along the crystallographic *a*-axis, alternating between inorganic and organic monolayers, as illustrated in Fig. 9(right). The ring interaction parameters of compounds **4** and **5**, as defined in PLATON,<sup>17</sup> are listed in Table 10, with  $d(\text{Cg}-\text{Cg}) < 6.0$  Å and  $\beta < 60^\circ$ . No non-covalent anion–aromatic interactions between the aromatic moieties and the halido ligands of the respective tetrahalometallates, as defined in PLATON,<sup>17</sup> are present.

### [acr-H]<sub>2</sub>[ZnX<sub>4</sub>] (**6**, **7**) and [acr-H]<sub>2</sub>[CdX<sub>4</sub>] (**8**, **9**)

Compounds **6–8** are isostructural and crystallise in the monoclinic space group C2/c. The asymmetric units of compounds **6–8** contain an M<sup>2+</sup> ion, coordinated to two halido ligands, and one isolated acridinium cation, with M = Zn<sup>2+</sup> in compounds **6** and **7** and M = Cd<sup>2+</sup> in compound **8**, as shown in Fig. 10(left).

Although compound **9** differs from compounds **6–8** in terms of unit cell dimensions and space group assignment and is thus not isostructural to the series, its composition is achieved by the replacement of the Zn<sup>2+</sup> ion in **7** with a Cd<sup>2+</sup> ion in **9**. The asymmetric unit of **9** comprises a Cd<sup>2+</sup> ion, coordinated to four bromido ligands, and two crystallographically independent, isolated acridinium cations, denoted as A and B for the cations containing atoms N1 and N3, respectively. Compound **9** crystallises in the space group P $\bar{1}$ . The crystallographic parameters of compounds **6–9** are listed in Table 1.

In compounds **6–8**, the M<sup>2+</sup> ion is located at (0, *y*, 3/4) in the unit cell. A two-fold rotation axis with direction [0, 1, 0] at (0, *y*, 1/4) generates the complete mononuclear tetrahedral complex anions for compounds **6–8**, as illustrated in Fig. 10(right). The local tetrahedral Cd<sup>2+</sup> and Zn<sup>2+</sup> coordination spheres in all compounds are formed by four halido ligands with  $\angle(\text{XMX})$ s and M–X bond distances collated in Table 4. The variation in bond angles of the tetrahalometallate anions is slightly larger in the Cd<sup>2+</sup> chlorido species **8**, ranging between 105.72(16)° and 116.72(17)°, compared to that observed in compounds **6**, **7** and **9**. The M–X bond lengths increase from the Zn<sup>2+</sup> anion to the Cd<sup>2+</sup> anion for a specific halido ligand, as well as with the size of the halido ligand for a specific metal ion.

**Table 4** M–X bond lengths and  $\angle(\text{XMX})$ s of tetrahalometallate units in **6–9** [Å and °]

<b>6</b>		<b>7</b>	
Zn(1)–Cl(1) <sup>#2</sup>	2.299(4)	Zn(1)–Br(2) <sup>#2</sup>	2.389(2)
Zn(1)–Cl(1)	2.299(4)	Zn(1)–Br(2)	2.389(2)
Zn(1)–Cl(2) <sup>#2</sup>	2.309(4)	Zn(1)–Br(1)	2.423(2)
Zn(1)–Cl(2)	2.309(4)	Zn(1)–Br(1) <sup>#2</sup>	2.423(2)
Cl(1) <sup>#2</sup> –Zn(1)–Cl(1)	107.0(2)	Br(2) <sup>#2</sup> –Zn(1)–Br(2)	114.01(15)
Cl(1) <sup>#2</sup> –Zn(1)–Cl(2) <sup>#2</sup>	106.92(17)	Br(2) <sup>#2</sup> –Zn(1)–Br(1)	108.28(6)
Cl(1)–Zn(1)–Cl(2) <sup>#2</sup>	109.87(16)	Br(2)–Zn(1)–Br(1)	109.45(6)
Cl(1) <sup>#2</sup> –Zn(1)–Cl(2)	109.87(16)	Br(2) <sup>#2</sup> –Zn(1)–Br(1) <sup>#2</sup>	109.45(6)
Cl(1)–Zn(1)–Cl(2)	106.92(17)	Br(2)–Zn(1)–Br(1) <sup>#2</sup>	108.28(6)
Cl(2) <sup>#2</sup> –Zn(1)–Cl(2)	116.0(2)	Br(1)–Zn(1)–Br(1) <sup>#2</sup>	107.16(14)



8		9	
Symmetry transformations used to generate equivalent atoms: <sup>#1</sup> -x, y, -z + 3/2, <sup>#2</sup> -x, y, -z + 1/2.			
Cl(1)–Cd(1)	2.472(3)	Br(1)–Cd(1)	2.5588(5)
Cl(2)–Cd(1)	2.430(3)	Br(2)–Cd(1)	2.5764(5)
Cd(1)–Cl(2) <sup>#1</sup>	2.430(3)	Br(3)–Cd(1)	2.6033(5)
Cd(1)–Cl(1) <sup>#1</sup>	2.472(3)	Br(4)–Cd(1)	2.5935(4)
Cl(2) <sup>#1</sup> –Cd(1)–Cl(2)	116.72(17)	Br(1)–Cd(1)–Br(2)	113.903(16)
Cl(2) <sup>#1</sup> –Cd(1)–Cl(1)	109.25(11)	Br(1)–Cd(1)–Br(4)	111.089(17)
Cl(2)–Cd(1)–Cl(1)	107.68(11)	Br(2)–Cd(1)–Br(4)	108.151(16)
Cl(2) <sup>#1</sup> –Cd(1)–Cl(1) <sup>#1</sup>	107.68(11)	Br(1)–Cd(1)–Br(3)	109.602(17)
Cl(2)–Cd(1)–Cl(1) <sup>#1</sup>	109.25(11)	Br(2)–Cd(1)–Br(3)	108.485(18)
Cl(1)–Cd(1)–Cl(1) <sup>#1</sup>	105.72(16)	Br(4)–Cd(1)–Br(3)	105.217(16)

In compounds **7** and **8**, with  $M = \text{Zn}^{2+}$ ,  $X = \text{Br}^-$  and  $M = \text{Cd}^{2+}$ ,  $X = \text{Cl}^-$ , respectively, the M–X bonds that are involved in strong  $\text{N}(1)\text{--H}(1\text{N}1)\cdots\text{X}(1)$  hydrogen bonding interactions, which connect the acridinium cations to the tetrahalometallate moieties, are the longest. This interaction is shown in Fig. 12 for compound **7**.

This is not the case in compound **6**, where the longest Zn–X bond distance corresponds to the halido ligands connected by weak hydrogen bonding to the ring hydrogen atoms of the acridinium ligands. The said strong  $\text{N}(1)\text{--H}(1\text{N}1)\cdots\text{X}(1)$  hydrogen bond distances increase with the size of the metal cations, as well as with the size of the halido ligands, in both the  $\text{Cd}^{2+}$  and  $\text{Zn}^{2+}$  series.

The acridinium cations in the isomorphous C2/c set of compounds are planar. Weak C–H $\cdots$ X–M hydrogen bonding contacts between the ring hydrogen atoms and the X(2) ligands of the mononuclear complexes further expand the structures parallel to the ac-plane as hydrogen-bonded strings that comprise alternating tetrahalometallate and double acridinium units, as depicted in Fig. 11(top) for compounds **6** and **8** and Fig. 12 for compound **7**, to finally form the layered structure shown in Fig. 11(bottom).

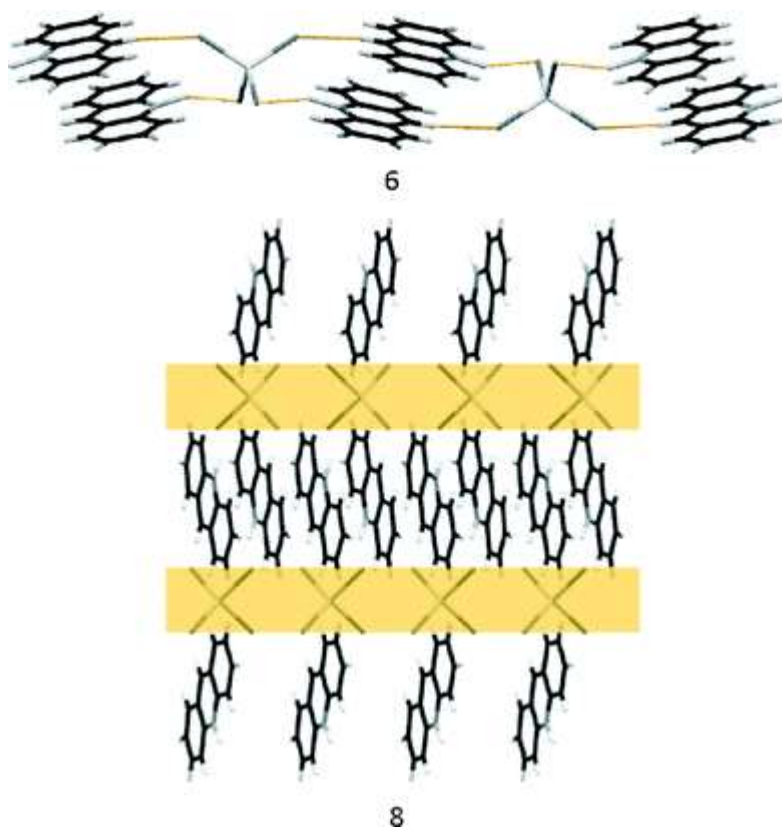


**Fig. 11** Both strong  $N(1)-H(1N1)\cdots Cl(1)$  and weak hydrogen bonding interactions between the organic and inorganic moieties in **6** (top). Packing of **8** viewed down the crystallographic *a*-axis in which the inorganic layers are highlighted in orange (bottom).



**Fig. 12** Hydrogen-bonded string in compound **7** formed by both strong  $N(1)-H(1N1)\cdots Cl(1)$  and weak hydrogen bonding interactions between the organic cations and the inorganic moieties.

The layered structure consists of alternating organic and inorganic monolayers parallel to the *ac*-plane. The tetrahalometallate moieties in the inorganic layers all pack with the same orientation in each layer, but alternate in orientation between successive layers, as illustrated in Fig. 11.

The acridinium cations in the organic layer are parallel to each other, but with alternating, head-to-tail orientation of the  $N(1)$  atom as dictated by both the  $N(1)-H(1N1)\cdots X(1)$  hydrogen bonds between the inorganic and organic layers and maximisation of van der Waals contacts between the aromatic organic moieties.

The acridinium cations in successive layers alternate in orientation, with the mean planes through the acridinium cations in consecutive organic layers at angles of  $38.60^\circ$ ,  $38.26^\circ$  and  $38.00^\circ$  to each other, in compounds **6–8**, respectively. Centroid-to-centroid and perpendicular slippage distances between the parallel acridinium ligands are given in Table 10.

Centroid-to-centroid distances alternate, with the largest distance, as dictated by the tetrahalometallate moiety, between the double acridinium units in the respective hydrogen-bonded strings described.

Even though structure **9** is composed of the same type of molecular ions, in the same ratio as that in structures **6–8**, the packing of the units is different, resulting in a structure which is not isostructural to the other three structures. The largest M–X distance in compound **9** corresponds to the Cd–Br(3) bond. The Br(3) ligand is, however, not an N–H···X–M hydrogen bond acceptor. Two weak C–H···X–M hydrogen bonding interactions between the ring hydrogen atoms, H(7) and H(20), on acridinium ligands A and B, respectively, and the Br(3) ligand are observed. C(7)–H(7) and C(20)–H(20) are positioned para to the amine functionalities in the respective acridinium ligands. Strong N(1)–H(1N1)···Br(4)–Cd and N(2)–H(1N2)···Br(2)–Cd hydrogen bonds exist between acridinium ligands A and B and the tetrahalometallate moiety.

These contacts connect the tetrahalometallate and acridinium moieties as a hydrogen-bonded string of successive inorganic and double organic units, as shown in Fig. 13 and listed in Table 9. The organic units consist of alternating acridinium ring AA and BB pairs.

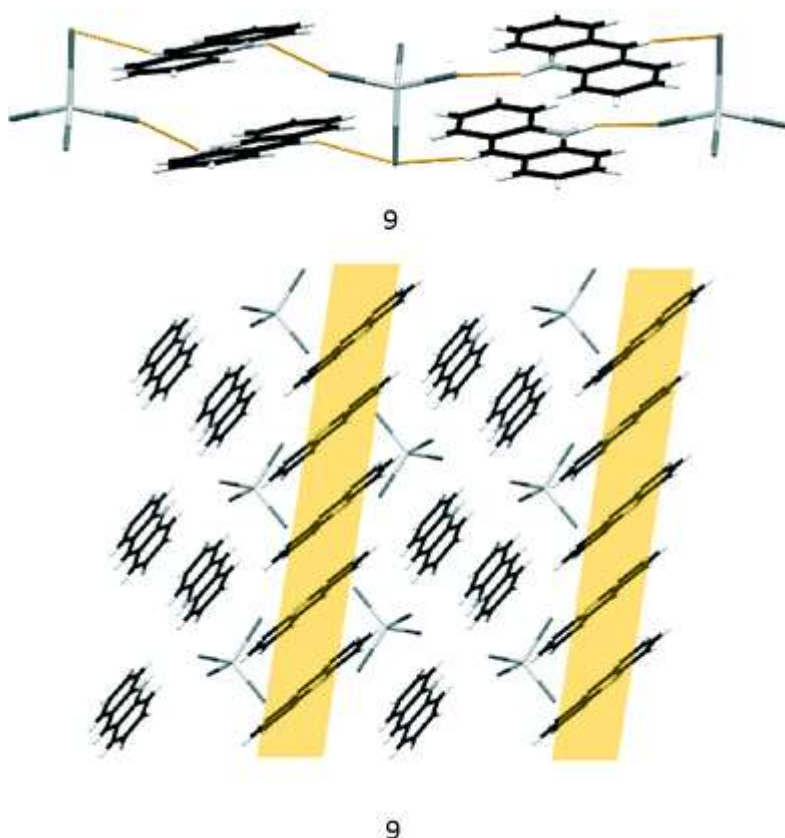


**Fig. 13** Both strong, charge-assisted and weak hydrogen bonding interactions between the organic and inorganic moieties in compound **9** (top). Packing viewed down the crystallographic b-axis (bottom) in which the organic monolayers are highlighted in orange.

The packing arrangement in compound **9** differs substantially from that observed in the C2/c set of compounds. Although both acridinium moieties are planar and the packing arrangement is layered, comprising alternating organic and inorganic layers parallel to the ac-

plane in structure **9**, the organic layers alternate between single and double layers, as illustrated in Fig. 13. The single layers consist of acridinium B cations which are in an offset stack arrangement,<sup>18</sup> parallel to each other, packing in a head-to-tail orientation. When viewed down the crystallographic a-axis, the acridinium A moieties, which comprise the double layers, are positioned lengthwise along the direction of the layer, parallel to each other, but alternating in orientation of the N–H group across the width of the double layer.

The orientation of the acridinium cations within both types of layers is such that the thickness of the organic layers, measured as the perpendicular distance between Cd<sup>2+</sup> metal centres across the organic layers, does not reflect the organic composition of the layer, due to the tilt angle of the cations. The thickness of the organic monolayer is 8.2832(6) Å while that of the double layer is 7.1074(5) Å.

Centroid-to-centroid distances between successive acridinium moieties are collated in Table 10. The centroid-to-centroid distance alternates between the BB acridinium pairs comprising the monolayer. The smallest centroid-to-centroid distance of 3.8353(19) Å is displayed between cations in the BB-units which are hydrogen-bonded to the same tetrahalometallate unit. The inter-unit BB distances are longer, having a value of 5.635(2) Å. The tetrahalometallate units comprising the inorganic monolayers all do, however, pack in the same orientation within the respective layer, but alternate in orientation between layers, as was the case in the C2/c series.

### [phe-H<sub>2</sub>]phe[ZnX<sub>4</sub>] (**10**)

Compound **10** is isomorphous with compounds **6–8** and crystallises in the monoclinic space group C2/c. As inferred from the difference Fourier synthesis and hydrogen bonding interactions, one phenazine molecule is protonated at both nitrogen atoms N(1) and N(2), yielding a phenazindium dication, and is denoted as ring A in further discussion, while the second phenazine molecule is not protonated at all and will be denoted as ring B. The asymmetric unit of **10** contains a Zn<sup>2+</sup> ion coordinated to two halido ligands, one phenazindium dication and half a neutral phenazine molecule, as shown in Fig. 14(left). The crystallographic parameters of compound **10** are listed in Table 1. In **10**, the Zn<sup>2+</sup> ion is located at (1, y, 3/4) in the unit cell. A two-fold rotation axis with direction [0, 1, 0] at (0, y, 1/4) generates the complete mononuclear tetrahedral complex, as illustrated in Fig. 14(right). The Zn<sup>2+</sup> ion is tetrahedrally coordinated by four halido ligands with the ∠(XZnX)s and Zn–X bond distances collated in Table 5. The X–Zn–X bond angles of the tetrahedral tetrahalometallate moiety fall between 112.01(4)° and 107.61(7)°.

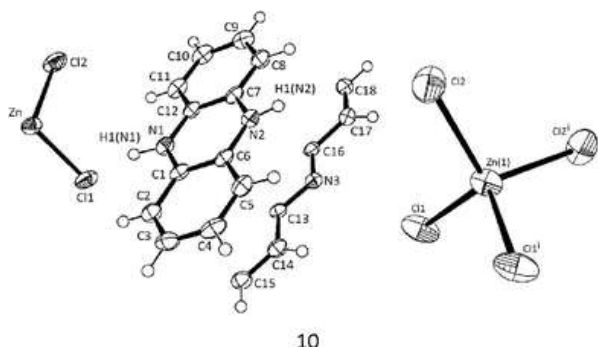


**Fig. 14** Asymmetric unit of **10**, showing the atomic numbering scheme (left). The complete mononuclear tetrahedral unit of **10** (right). Displacement ellipsoids are shown at the 30% probability level and hydrogen atoms are shown as small spheres of arbitrary radii.

**Table 5** Zn–Cl bond lengths and  $\angle(\text{ClZnCl})$ s of the tetrachlorozincate unit in **10** [Å and °]

<b>10</b>		<b>Symmetry operator</b>
Zn–Cl(1) <sup>#1</sup>	2.2610(11)	<sup>#1</sup> $-x + 2, y, -z + 3/2$
Zn–Cl(1)	2.2610(11)	
Zn–Cl(2)	2.2696(12)	
Zn–Cl(2) <sup>#1</sup>	2.2697(12)	
Cl(1) <sup>#1</sup> –Zn–Cl(1)	109.42(6)	
Cl(1) <sup>#1</sup> –Zn–Cl(2)	112.01(4)	
Cl(1)–Zn–Cl(2)	107.91(4)	
Cl(1) <sup>#1</sup> –Zn–Cl(2) <sup>#1</sup>	107.91(4)	
Cl(1)–Zn–Cl(2) <sup>#1</sup>	112.01(4)	
Cl(2)–Zn–Cl(2) <sup>#1</sup>	107.61(7)	

Both organic moieties are planar and the full phenazine molecule **B** is generated by an inversion center at [0, 0, 0]. Since all four halido ligands in the tetrachlorozincate moiety of compound **10** are involved in strong N(1)–H(1N1)···Zn(1) hydrogen bonding with the doubly protonated phenazindium dications, the Zn–Cl bond distances vary very little, with the slightly larger bond distances corresponding to the Zn–Cl bonds involved in both strong and weak hydrogen bonding interactions from the same organic dication.

Weak C(8)–H(8)···Cl(2) hydrogen bonds together with strong charge-assisted N–H···X–M hydrogen bonds connect the phenazindium dications and the inorganic units diagonally across the ac-plane as a hydrogen-bonded zigzag string that comprises tetrahalometallate nodes connected by two parallel phenazindium units as depicted in Fig. 15, and hydrogen bonding parameters are listed in Table 9. The centroid-to-centroid distance between the parallel AA-units is 3.254(2) Å, while the angle between the mean planes of successive interchain phenazindium cation pairs is close to orthogonal, having a value of 89.35°. Aromatic interactions are listed in Table 10. Short C(18)–H(18)···Cl(1)–Zn(1) hydrogen contacts between the B cation units and the tetrahalometallate units of 2.948 Å form another zigzag string parallel to the bc-plane. In this string, the inorganic moieties again form the nodes, but the organic linkers are, in this case, single B-units, as illustrated in Fig. 16. Alternate B-units are not parallel, with the mean planes through the phenazine molecules at an angle of 84.58° to each other. The two hydrogen-bonded strings, string A and string B, are not isolated from one another, but engage by forming interlocking S-shaped hydrogen-bonded motifs. The B-unit represents the middle bar of the letter ‘S’, while two single A-units form the top and bottom bars of the letter. The bars are further linked by weak C(18)–H(18)···Cl(1)–Zn(1) and C(3)–H(3)···Cl(2)–Zn(1) short hydrogen bonding contacts to the tetrahalometallate moieties, which then represent the curves of the letter, as illustrated in Fig. 17. The B-unit therefore slots in between successive AA-units in an AABAABAA pattern. The interdigitated B-unit is not parallel to the neighbouring AA-units, but slightly offset at an angle of 2.86(17)°. The centroid-to-centroid distance between the A- and B-units of the S-shaped motif is 3.582(2) Å, and since the two units are not parallel, the slippage distance cannot be reported.

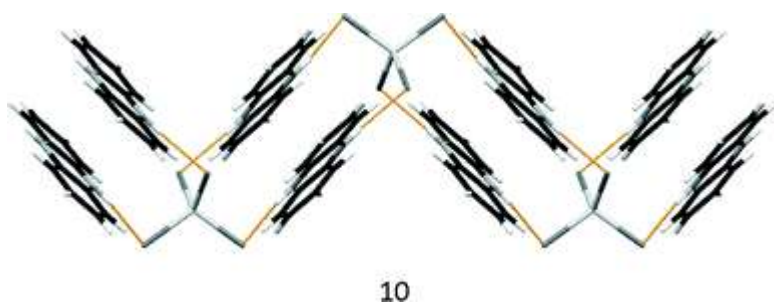


**Fig. 15** Strong charge-assisted N(1)–H(1N1)⋯Cl–Zn hydrogen bonding between the phenazindium cations and inorganic moieties in **10**, forming a one-dimensional hydrogen-bonded zigzag string, as viewed along the crystallographic c-axis.

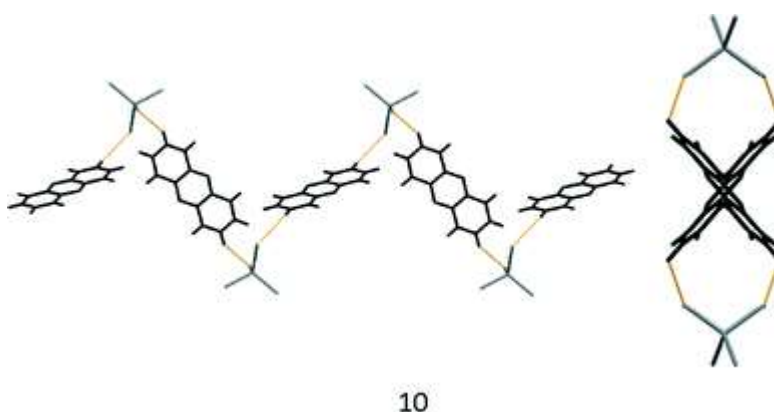


**Fig. 16** Weak C(18)–H(18)⋯Cl short hydrogen bonding contacts between the phenazine molecules and inorganic anions in **10**, as viewed along the crystallographic a-axis (left) and c-axis (right).

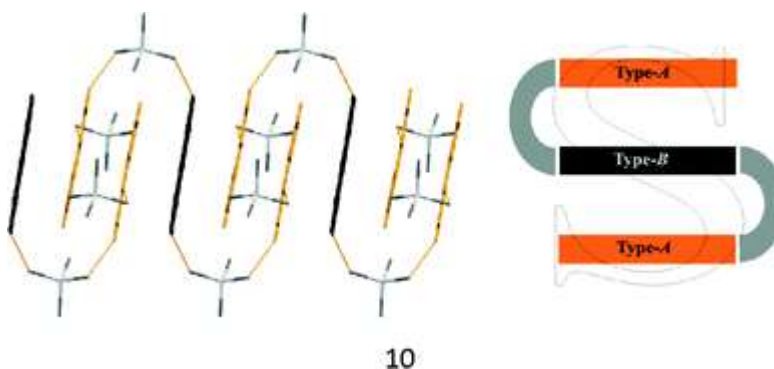
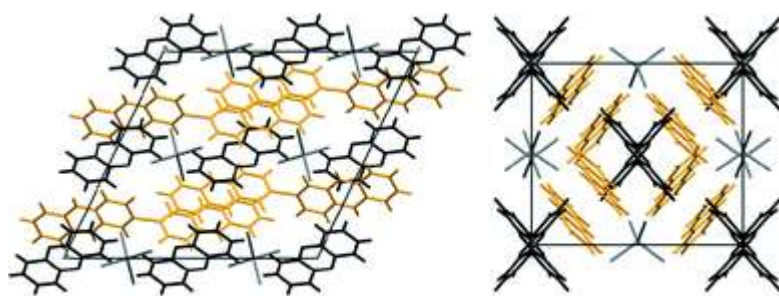


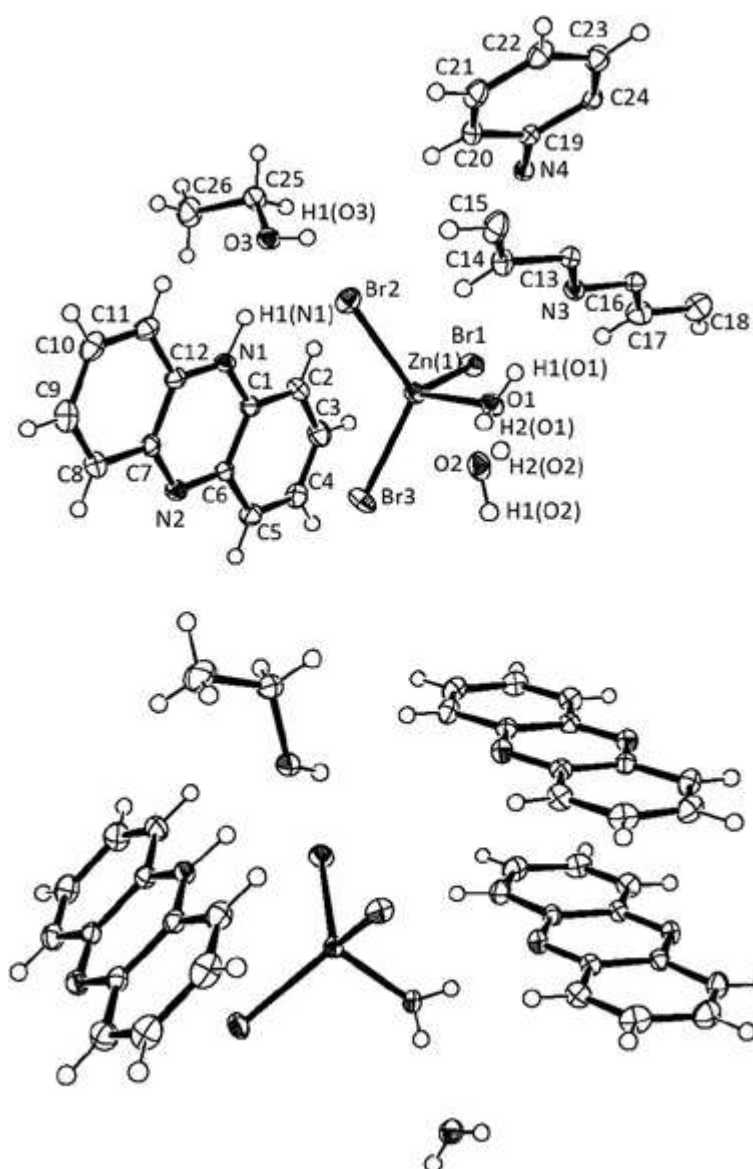
**Fig. 17** Interlocking between the A- and B-type units via short hydrogen bonding contacts and aromatic interactions (left). Schematic illustration of the S-shaped motif formed (right). The A-type units are indicated in orange with the B-type units in black.

The packing is layered and consists of alternating organic and inorganic monolayers parallel to the bc-plane. The organic layer is a thick monolayer due to the different orientations of the A and B components within the layer. The tetrahalometallate moieties in the inorganic layers all pack with the same orientation in each layer, but alternate in orientation between successive layers, as can be seen from the packing arrangement viewed down the crystallographic c-axis in Fig. 18(right).



10

**Fig. 18** Packing arrangement of **10** as viewed down the crystallographic b- (left) and c-axes (right). The A-type units are indicated in orange with the B-type units in black.



11

**Fig. 19** Asymmetric unit of **11**, showing the atomic numbering scheme (top). The complete mononuclear tetrahedral unit of **11** with full symmetry-generated organic moieties (bottom). Displacement ellipsoids are shown at the 50% probability level and hydrogen atoms are shown as small spheres of arbitrary radii.



## [phe-H](phe)<sub>2</sub>[Zn(OH<sub>2</sub>)Br<sub>3</sub>]·EtOH·H<sub>2</sub>O (**11**)

Compound **11** crystallises in the triclinic space group  $P\bar{1}$ . The asymmetric unit of **11** contains a Zn<sup>2+</sup> ion tetrahedrally coordinated by three bromido ligands and one aqua ligand, as shown in Fig. 19. The asymmetric unit also contains one complete phenazinium cation and two halves of two crystallographically independent neutral phenazine molecules together with an ethanol and a water molecule, both of which are isolated. The phenazine moieties will be denoted as A, B and C, indicating species containing atoms N(1), N(3) and N(4), respectively. The crystallographic parameters of compound **11** are listed in Table 1.

In **11**, all atoms lie on general positions. The complete organic moieties of B and C are generated by operation of an inversion centre at [0, 0, 0]. Only ring A is protonated at the N(1) atom to give the phenazinium cation, while rings B and C are neutral molecules. The hydrogen atoms of the aqua ligand coordinated to the Zn<sup>2+</sup> cation, the isolated water molecule as well as the hydroxyl functionality were generated with the program CALC-OH by Nardelli.<sup>19</sup> The local tetrahedral Zn<sup>2+</sup> coordination sphere is coordinated by three bromido ligands and one water molecule, with  $\angle(XZnX)$ s and Zn–X bond distances ranging between 102.50(3)° and 116.894(9)° and 2.3666(2) Å and 2.4012(2) Å, respectively, as collated in Table 6. The rather large variation in tetrahedral bond angles of the inorganic Zn<sup>2+</sup> moiety is ascribed to the difference in steric and electronic requirements of the coordinated ligands, where the angles involving the O(1) atom are smaller. The shortest bond distance also belongs to the Zn–O(1) bond.

**Table 6** M–X bond distances and  $\angle(XMX)$ s of the tetrahalometallate unit in **11** [Å and °]

<b>11</b>	
Zn–O(1)	2.0198(10)
Zn–Br(3)	2.3666(2)
Zn–Br(2)	2.3897(2)
Zn–Br(1)	2.4012(2)
O(1)–Zn–Br(3)	104.40(3)
O(1)–Zn–Br(2)	102.50(3)
Br(3)–Zn–Br(2)	116.894(9)
O(1)–Zn–Br(1)	103.14(3)
Br(3)–Zn–Br(1)	113.347(8)
Br(2)–Zn–Br(1)	114.268(8)

In compound **11**, the tetrahedral inorganic moiety is connected to the isolated water molecule by strong O(1)–H(2O1)···O(2) hydrogen bonds between one of the hydrogen atoms of the coordinated water ligand and the oxygen atom of the isolated water molecule. This links the two units into a hydrogen-bonded string along the crystallographic a-axis, as indicated in Fig. 20(top). All hydrogen bonding interactions are listed in Table 9. Further expansion via only strong hydrogen bonds results in the formation of a wave-like chain, as illustrated in Fig. 20(middle), in which strong O(3)–H(1O3)···O(2) hydrogen bonds between the hydroxyl hydrogen atom of the ethanol molecule and the oxygen atom of the isolated water molecule are formed, resulting in the wave-like motif in which the ethanol molecule represents the crests of the waves. Incorporation of weak hydrogen bonds allows extraction of another hydrogen-bonded motif, as illustrated in Fig. 20(bottom). This motif can be described as a knotted string, in which the final tie of the knot is formed by weak C(25)–H(25A)···Br(3) hydrogen bonds. The isolated water molecule is further hydrogen-bonded to phenazine ring



C, via O(2)–H(2O2)···N(4) hydrogen bonds, while the second hydrogen atom of the coordinated water molecule is connected to phenazine ring B, through O(1)–H(1O1)···N(3) hydrogen bonds. Finally, the phenazinium cation is connected to the ethanol molecule by strong charge-assisted N(1)–H(1N1)···O(3) hydrogen bonding to complete the thick strong hydrogen-bonded string, as illustrated in Fig. 21(left).

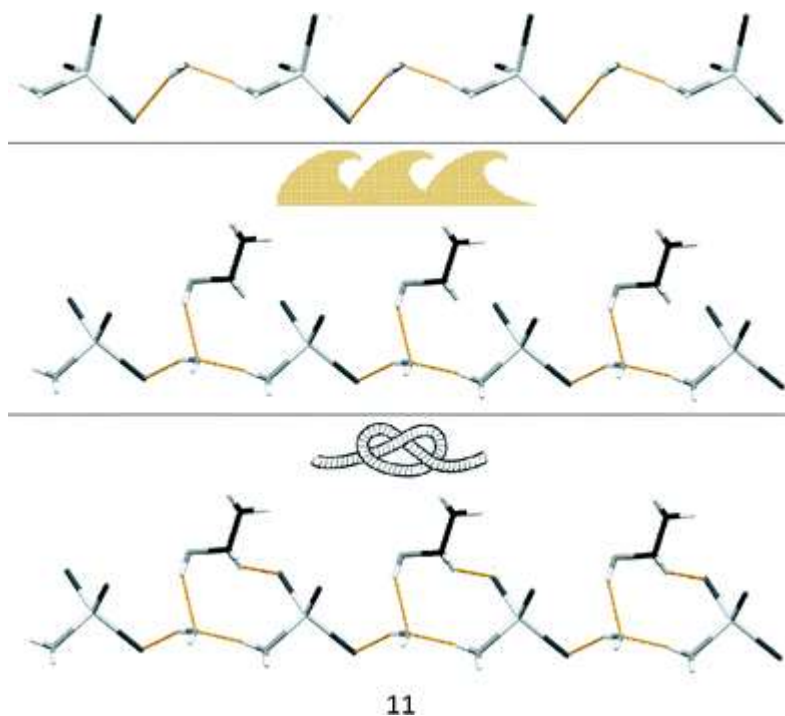


**Fig. 20** Hydrogen-bonded string formed by alternating tetrahalometallate and water molecules, as viewed along the crystallographic c-axis (top). Wave-like motif adopted by the said string upon incorporation of strong hydrogen bonds from the hydroxyl hydrogen of the ethanol molecule (middle). Knotted-string motif extracted upon consideration of weak hydrogen bonding interactions (bottom).

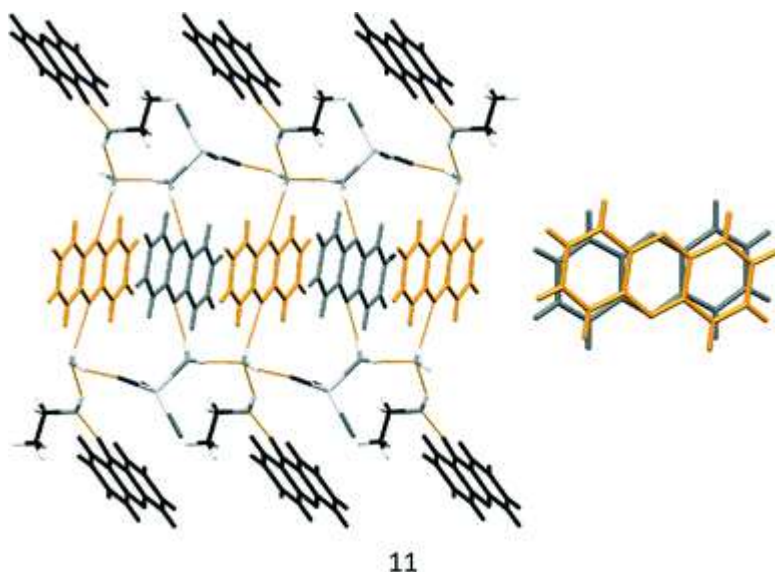


**Fig. 21** Extension of the hydrogen-bonded string via strong hydrogen bonds, viewed orthogonal to the direction of string propagation (left). The lacing phenazinium cation A is indicated in black, with the phenazine molecules B and C shown in grey and orange, respectively. Phenazine molecules B (grey) and C (orange) slightly tilted and rotated relative to one another (right).

The thick hydrogen-bonded string therefore comprises two inorganic chains, separated by a monolayer of alternating B and C molecules and laced by the phenazinium cations A. The centroid-to-centroid distance between the BC units is 3.8760(8) Å, and although the molecules are not completely parallel, with the respective mean planes at an angle of 0.90°, they are however, at 8.99°, slightly rotated relative to one another to achieve maximum van der Waals contacts between the rings, as illustrated in Fig. 21(right).

Weak hydrogen bonding interactions, together with aromatic interactions, further connect the strong hydrogen-bonded chains in a direction orthogonal to that of chain propagation to obtain the arrangement illustrated in Fig. 22(bottom), in which the different hydrogen-bonded chains are indicated in orange and black. The interlocking aromatic unit is shown in Fig. 22(top). Weak C(8)–H(8)⋯Br(3) and C(4)–H(4)⋯Br(3) hydrogen bonds of 2.9825 Å and 2.9878 Å, respectively, together with aromatic interactions between interdigitated phenazinium cations, stabilise the interlocking unit as indicated in Fig. 22(bottom). The centroid-to-centroid distance between the parallel phenazinium cations is 3.7242(8) Å, with a perpendicular slippage distance of 1.454 Å. All ring interaction parameters are collated in Table 10. The interdigitated phenazinium cations alternate in orientation of the protonated N(1) atom as dictated by the N(1)–H(1N1)⋯O(3) hydrogen bonds in adjacent thick layers. Interlocking of the different thick layers does not, however, obscure the repeating interlocking units, as they remain identifiable upon combination of the adjacent chains, as indicated in Fig. 22(bottom).

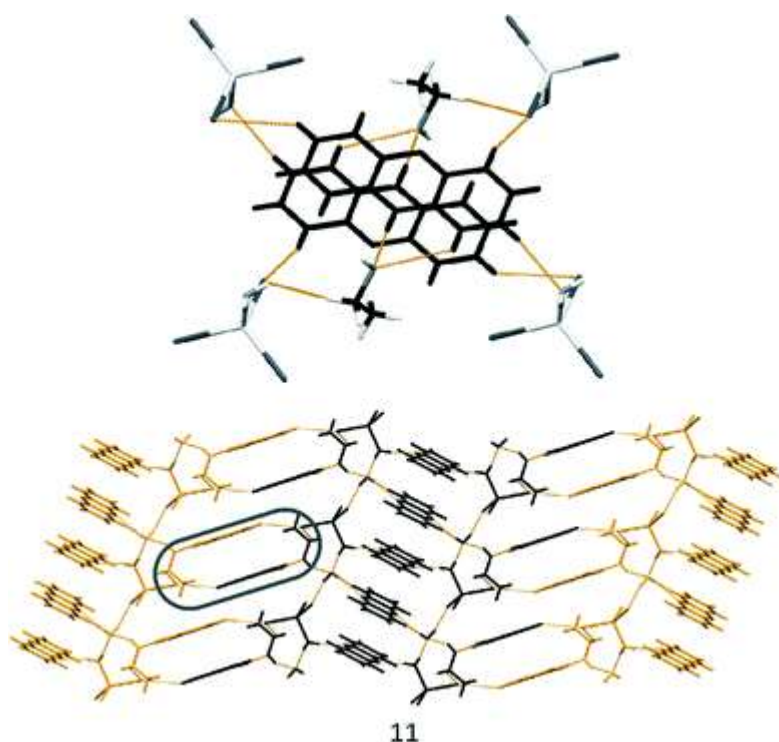
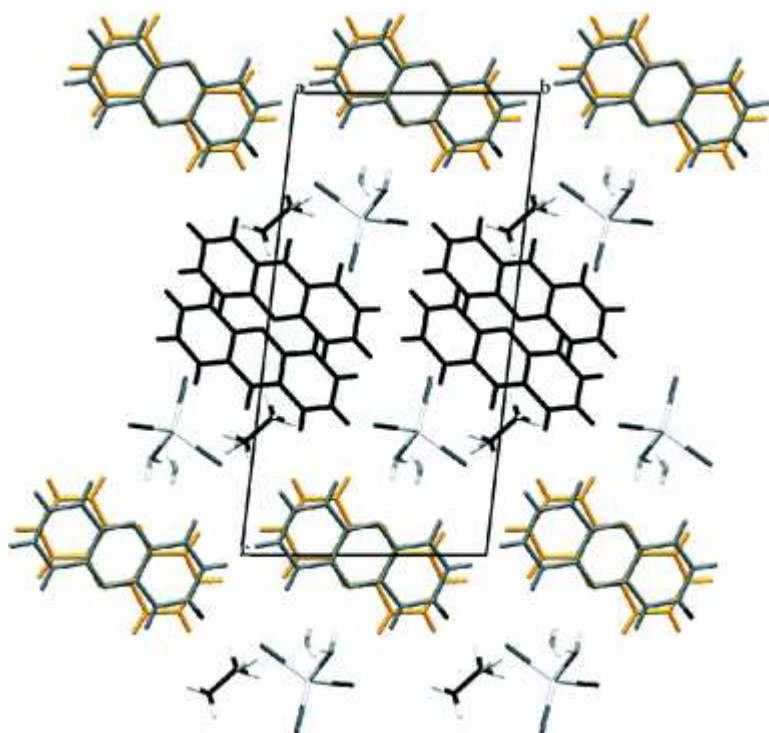


**Fig. 22** Interlocking unit between adjacent thick hydrogen-bonded chains, with the phenazinium cations indicated in black. Interlocked chains with an interlocking unit indicated. Adjacent thick chains are highlighted in alternating colours of black and orange.

In addition to the described hydrogen bonding and aromatic interactions, further non-covalent anion–aromatic interactions between the aromatic moieties and the X(1) and X(4) halido ligands of the respective tetrahalometallates are present. All anion–aromatic interactions, as defined in PLATON,<sup>17</sup> are collated in Table 11. As illustrated in Fig. 23, the packing

arrangement of compound **11** is layered, forming alternating organic and inorganic layers. The organic layers alternate in composition from layer to layer, forming a monolayer composed of phenazine units B and C, alternating with an inorganic layer consisting of phenazinium cations A only. The width of the organic layers, measured as the distance between the Zn<sup>2+</sup> centres in the different layers, indicates that the BC layer (12.2473 Å) is thicker than the A layer with a thickness of 9.0958 Å.



**11**

**Fig. 23** Packing arrangement of **11** as viewed along the crystallographic a-axis. The phenazinium cations A are indicated in black, with the phenazine molecules B and C shown in grey and orange, respectively.

**(phe)<sub>2</sub>[Zn(OH<sub>2</sub>)<sub>2</sub>X<sub>2</sub>]·H<sub>2</sub>O (12 and 13), (acr)<sub>3</sub>[Zn(OH<sub>2</sub>)<sub>2</sub>X<sub>2</sub>] (14) and (acr)<sub>3</sub>[Zn(OH<sub>2</sub>)X<sub>2</sub>(sv)] (15 and 16)**

Compounds **12** and **13** were prepared without acid present during crystallisation, hence the organic species are not protonated. Compounds **12** and **13** are isostructural, with the asymmetric units containing a Zn<sup>2+</sup> ion coordinated by two halido ligands and two aqua ligands, one isolated water molecule and two crystallographically independent phenazine molecules denoted as A and B for the rings containing atoms N(1) and N(3), respectively. Compounds **12** and **13** crystallise in the monoclinic space group P2<sub>1</sub>/c. Compounds **14** to **16** differ from compounds **12** and **13** in terms of unit cell dimensions and space group, with one of the structural differences being the replacement of the two phenazine molecules with three crystallographically independent acridine molecules, denoted as C, D and E for the ring systems containing atoms N(1), N(2) and N(3), respectively. The other structural difference lies in the ligands coordinated to the tetrahedral inorganic moieties. Compound **14** comprises a Zn<sup>2+</sup> cation coordinated by two halido ligands and two aqua ligands, while in compound **15** one of the coordinated aqua ligands is replaced by a coordinated O-isopropanol ligand and in compound **16** it is replaced by an O-ethanol ligand. Compounds **14** to **16** also do not contain isolated water molecules, as was the case in compounds **12** and **13**. In compounds **12** to **16**,

all atoms lie on general positions. Compounds **14** to **16** crystallise in the monoclinic space group  $P2_1/n$ . The crystallographic parameters of compounds **12** to **16** are listed in Table 1, and asymmetric units are shown in Fig. 24.

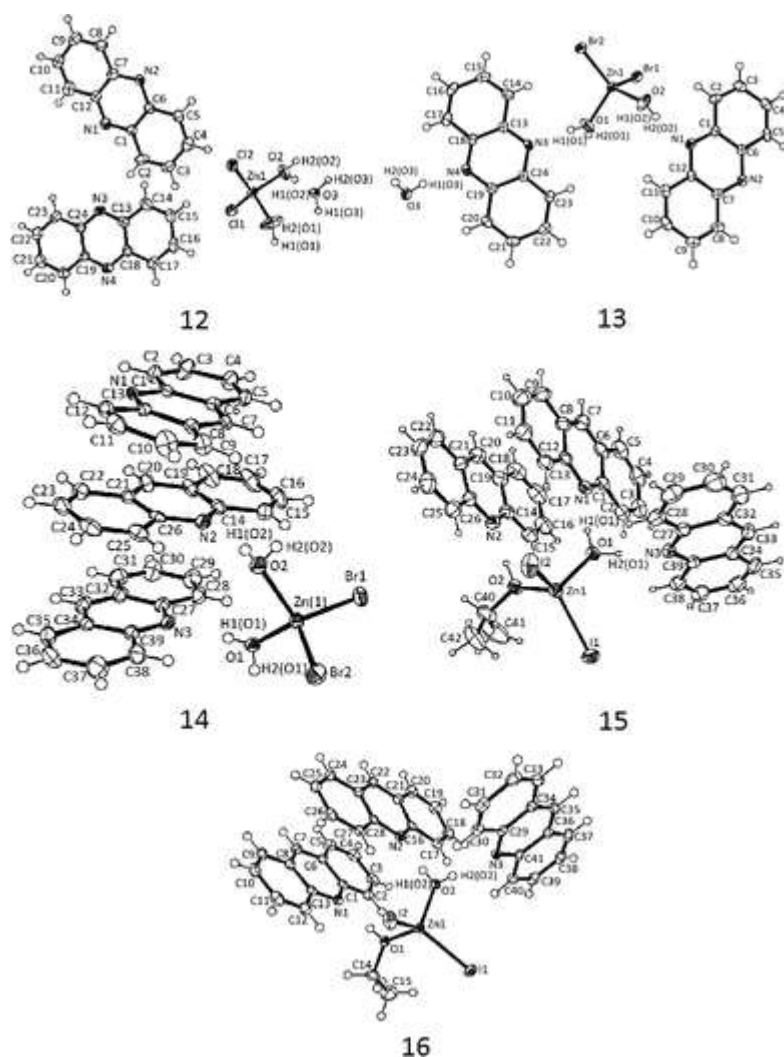


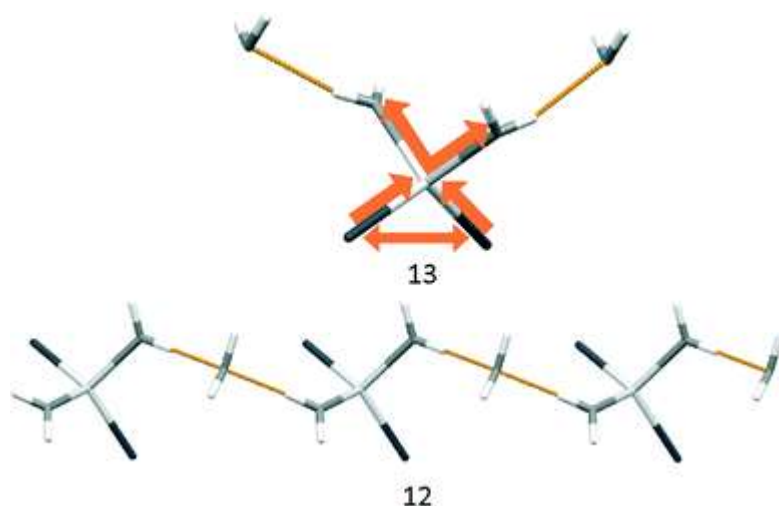
**Fig. 24** Asymmetric units of **12** to **16**, showing the atomic numbering scheme. Displacement ellipsoids are shown at the 50% probability level and hydrogen atoms are shown as small spheres of arbitrary radii.

The  $Zn^{2+}$  ion in all compounds is tetrahedrally coordinated by two halido (X) ligands and two O-donor (L) ligands, with all  $\angle(X/L-Zn-X/L)$ s and  $Zn-X/L$  bond distances collated in Table 7. The  $Zn-X$  distances (where  $X = \text{halido ligand}$ ) within the tetrahedral moieties increase predictably with the size of the halido ligand from **12** to **16**, with compound **12** having the shortest  $Zn-X$  distance of 2.195(3) Å, where  $X$  is a chlorido ligand, and compound **16** having the largest  $Zn-X$  distance of 2.5634(3) Å, where  $X$  is an iodido ligand. Upon comparing the two structurally identical tetrahedral moieties in compounds **13** and **14**, it is found that the  $Zn-O$  distances in **13** are elongated relative to the same distances in **14**, while the opposite holds true for the  $Zn-Br$  distances, which are shorter in **13**. This is accounted for by the presence of the isolated water molecule in compound **13**, of which the oxygen atom acts as a hydrogen bond acceptor from one of the coordinated aqua ligands in **13**, to form  $O(1)-H(2O1)\cdots O(3)$  hydrogen bonds, which has the effect of elongating the participating  $Zn-O$  bond. This also accounts for the larger  $X-Zn-X$  angles of  $123.86(12)^\circ$  and  $121.31(4)^\circ$  observed in compounds **12** and **13**, respectively, as schematically explained in Fig. 25(top).

**Table 7** M–X bond distances and  $\angle(\text{XMX})$ s of the tetrahalometallate units in **12–16** [ $\text{\AA}$  and  $^\circ$ ]

<b>12</b>		<b>13</b>		<b>14</b>	
Zn(1)–Cl(1)	2.195(3)	Zn(1)–Br(2)	2.3331(10)	Zn–Br(2)	2.3505(7)
Zn(1)–Cl(2)	2.206(3)	Zn(1)–Br(1)	2.3353(10)	Zn–Br(1)	2.3903(7)
Zn(1)–O(1)	1.991(9)	Zn(1)–O(1)	1.985(6)	Zn–O(1)	1.947(3)
Zn(1)–O(2)	1.996(9)	Zn(1)–O(2)	1.986(5)	Zn–O(2)	1.986(3)
O(1)–Zn(1)–O(2)	102.6(5)	O(1)–Zn(1)–O(2)	101.2(3)	O(1)–Zn–O(2)	98.80(14)
O(1)–Zn(1)–Cl(1)	109.1(3)	O(1)–Zn(1)–Br(2)	110.89(18)	O(1)–Zn–Br(2)	115.37(9)
O(2)–Zn(1)–Cl(1)	106.1(3)	O(2)–Zn(1)–Br(2)	106.52(18)	O(2)–Zn–Br(2)	109.76(10)
O(1)–Zn(1)–Cl(2)	105.9(3)	O(1)–Zn(1)–Br(1)	106.4(2)	O(1)–Zn–Br(1)	104.21(9)
O(2)–Zn(1)–Cl(2)	107.3(3)	O(2)–Zn(1)–Br(1)	108.73(18)	O(2)–Zn–Br(1)	111.56(10)
Cl(1)–Zn(1)–Cl(2)	123.86(12)	Br(2)–Zn(1)–Br(1)	121.31(4)	Br(2)–Zn–Br(1)	115.81(2)

<b>15</b>		<b>16</b>	
Zn(1)–I(1)	2.5562(5)	Zn(1)–I(1)	2.5542(2)
Zn(1)–I(2)	2.5594(5)	Zn(1)–I(2)	2.5634(3)
Zn(1)–O(1)	1.964(2)	Zn(1)–O(1)	1.9950(13)
Zn(1)–O(2)	2.000(2)	Zn(1)–O(2)	1.9472(13)
O(1)–Zn(1)–O(2)	100.47(11)	O(2)–Zn(1)–O(1)	101.65(6)
O(1)–Zn(1)–I(1)	104.63(8)	O(2)–Zn(1)–I(1)	106.72(4)
O(2)–Zn(1)–I(1)	111.35(8)	O(1)–Zn(1)–I(1)	107.74(4)
O(1)–Zn(1)–I(2)	109.60(9)	O(2)–Zn(1)–I(2)	110.44(4)
O(2)–Zn(1)–I(2)	111.27(9)	O(1)–Zn(1)–I(2)	111.05(4)
I(1)–Zn(1)–I(2)	117.85(2)	I(1)–Zn(1)–I(2)	117.927(9)

**Fig. 25** Zn–O) bond elongation via hydrogen bonding in compound **13** (top). Inorganic hydrogen-bonded string formation along the crystallographic a-axis in compound **12** (bottom).

The tetrahedral environments in compounds **15** and **16** both have two iodido ligands and one aqua ligand coordinated to the metal centre. The fourth position of the tetrahedral coordination sphere is satisfied by coordination of an O-isopropanol and O-ethanol ligand in

**15** and **16**, respectively. The coordinated alcohols correlate with the solvents used in the reaction procedure. The coordinated solvent molecules can be accounted for by considering the size and concomitant steric requirement of the coordinated iodido ligands. In both instances, the coordination of one alcoholic ligand, instead of two aqua ligands, creates more ‘space’ in the tetrahedral coordination sphere of the zinc(II) metal centre, by having the respective Zn–O bonds elongated relative to the Zn–OH<sub>2</sub> bond distances measured to be 2.000(2) Å and 1.9950(13) Å, respectively, and their coordination is therefore favoured.

Both **12** and **13** form an inorganic hydrogen-bonded string along the crystallographic a-axis, as illustrated in Fig. 25(bottom) for compound **12**, with the distance between adjacent Zn<sup>2+</sup> metal centres of 6.94010(10) Å and 6.9170(7) Å in **12** and **13**, respectively, equal to the a unit cell dimension. In compound **14**, the additional isolated water molecule is not available for hydrogen-bonded string formation, and the inorganic tetrahedral moieties form hydrogen-bonded dimers, as illustrated in Fig. 26. The tetrahedral moieties in compounds **15** and **16** also form pairs, but since no formal interaction exists between the pairs, they are referred to as dimeric associates, as illustrated in Fig. 27. The comprising mononuclear molecules in compounds **14** to **16** are symmetry-related by operation of an inversion centre.



Fig. 26 Hydrogen-bonded dimer formed by tetrahedral moieties in compound **14**.

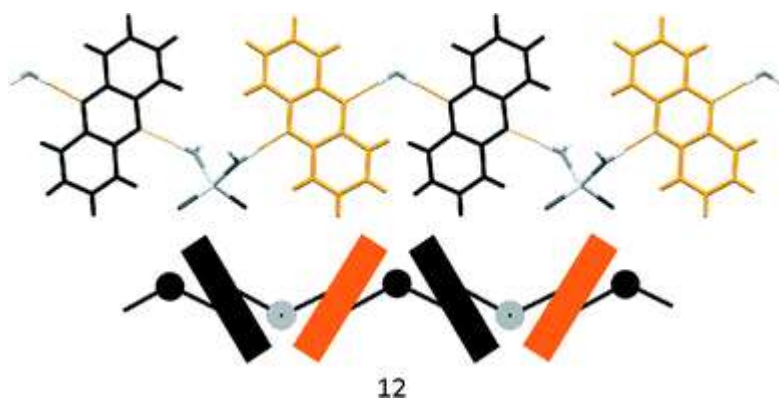


Fig. 27 Dimeric associated tetrahedral moieties in compounds **15** (left) and **16** (right).

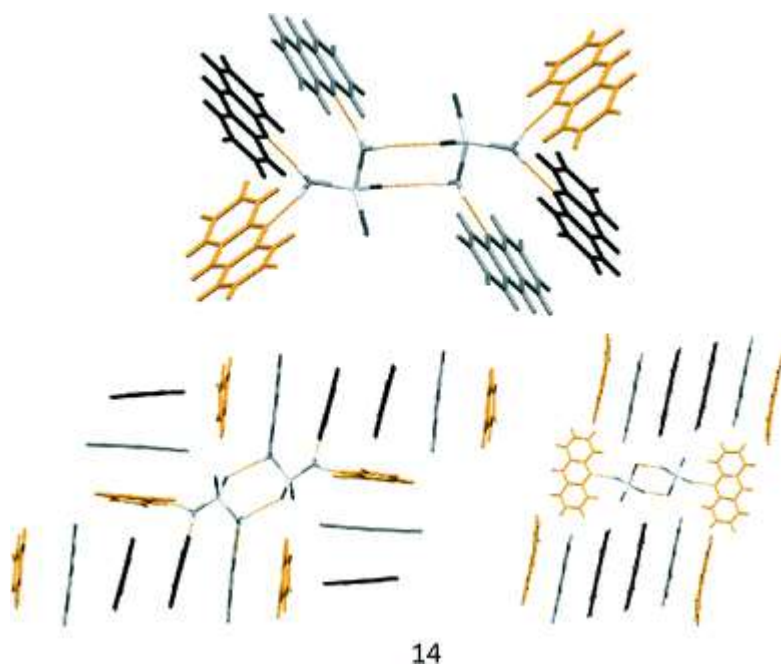
Compounds **12** and **13** are, in addition to the hydrogen-bonded inorganic strings along the direction of the crystallographic a-axis, also connected via hydrogen bonds along the crystallographic b-axis to form two-dimensional hydrogen-bonded sheets. In this organic–inorganic connection, alternating A and B organic molecules link alternating Zn<sup>2+</sup> and water moieties in the adjacent inorganic strings, as illustrated in Fig. 28(top) for **12**, where phenazine ring A is indicated in orange and phenazine ring B in black. Hydrogen bonding is realised from both inorganic units such that the hydrogen atom on the isolated water molecule forms O(3)–H(19)⋯N(1) and O(3)–H(20)⋯N(3) hydrogen bonds to phenazine molecules A (orange) and B (black), respectively. The nitrogen atom of B further acts as an O(1)–H(22)⋯N(4) hydrogen bond acceptor from the hydrogen atom on the O(1)–aqua ligand



coordinated to the  $Zn^{2+}$  moiety in an adjacent inorganic chain. The hydrogen atom on the O(2)–aqua ligand coordinated to the same  $Zn^{2+}$  metal centre forms another O(2)–H(24)···N(2) hydrogen bond to the nitrogen atom of A to propagate the sequence as schematically illustrated in Fig. 28(bottom). The dimeric inorganic units in compound **14** are isolated by being completely surrounded in all dimensions by the acridine molecules, as illustrated in Fig. 29(bottom). The dimer has three hydrogen atoms per inorganic unit remaining available to form strong hydrogen bonds to the nitrogen atoms in the different surrounding acridine molecules C, D and E. The rings are in turn electrostatically oriented around each dimeric unit, as illustrated in Fig. 29(top), to accept the respective O(1)–H(2O1)···N(1), O(1)–H(1O1)···N(3) and O(2)–H(1O2)···N(2) hydrogen bonds. The crystallographically independent acridine molecules are colour-coded in Fig. 29, with acridine molecules C, D and E coloured orange, grey and black, respectively. All hydrogen bonding parameters are collated in Table 9. Extension of the structure via weak C(2)–H(2)···Br(2) and C(15)–H(15)···Br(1) hydrogen bonds and aromatic interactions between the ring systems results in the arrangement illustrated in Fig. 29(bottom), in which the inorganic dimer is completely contained in a hydrophobic pocket created by acridine stacks of different orientations.



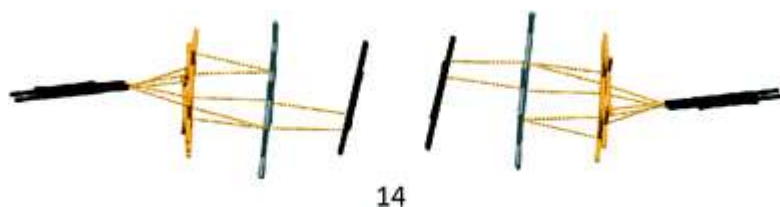
**Fig. 28** Two-dimensional hydrogen-bonded sheet formation along the crystallographic b-axis in compound **12** (top), with phenazine rings A and B coloured in orange and black. Schematic illustration of the hydrogen bond connectivity along the [0, 1, 0] direction in compound **12** (bottom), with grey and black spheres representing the water molecules and the tetrahedral inorganic moieties, respectively, and the dark grey and orange rods indicating phenazine rings B and A, respectively.



14

**Fig. 29** Hydrophobic environment created by six strong hydrogen bonds radiating from the dimeric unit to the aromatic rings in **14** (top). Extension of aromatic interactions which shows the stacking sequence of the aromatic rings and complete hydrophobic encapsulation of the dimer viewed from different angles (bottom). Acridine molecules C, D and E are coloured orange, grey and black, respectively.

One stack comprises three acridine molecules arranged in an inverted repeat CDEEDC sequence in which one CDE unit is symmetry-related to the next. The encapsulated arrangement holds true when different views of the hydrophobic pocket are considered, as illustrated in Fig. 29(bottom right). The aromatic acridine molecules comprising the CDE units are not parallel to each other, although the arrangement is such that aromatic interactions occur, as indicated in Fig. 30. The angles between the mean planes through C and D and D and E are measured to be  $3.76^\circ$  and  $8.21^\circ$ , respectively, while the in-plane rotation, which affords maximum van der Waals contacts between neighbouring moieties, have values of  $-139.01^\circ$  for the CD and  $-27.66^\circ$  for the DE pair. All ring interaction parameters are collated in Table 10. Symmetry generation of E via a glide plane perpendicular to the b-direction affords a favourable edge-to-face or T-shaped arrangement between moieties C and E, with the C(33)–H(33)⋯Cg(N1) distance of 2.88 Å. The ring puckering amplitude of 0.247(4) Å observed in the 14-membered ring of C is ascribed to this interaction. All X–H⋯Cg (aromatic ring) interaction parameters are listed in Table 12.



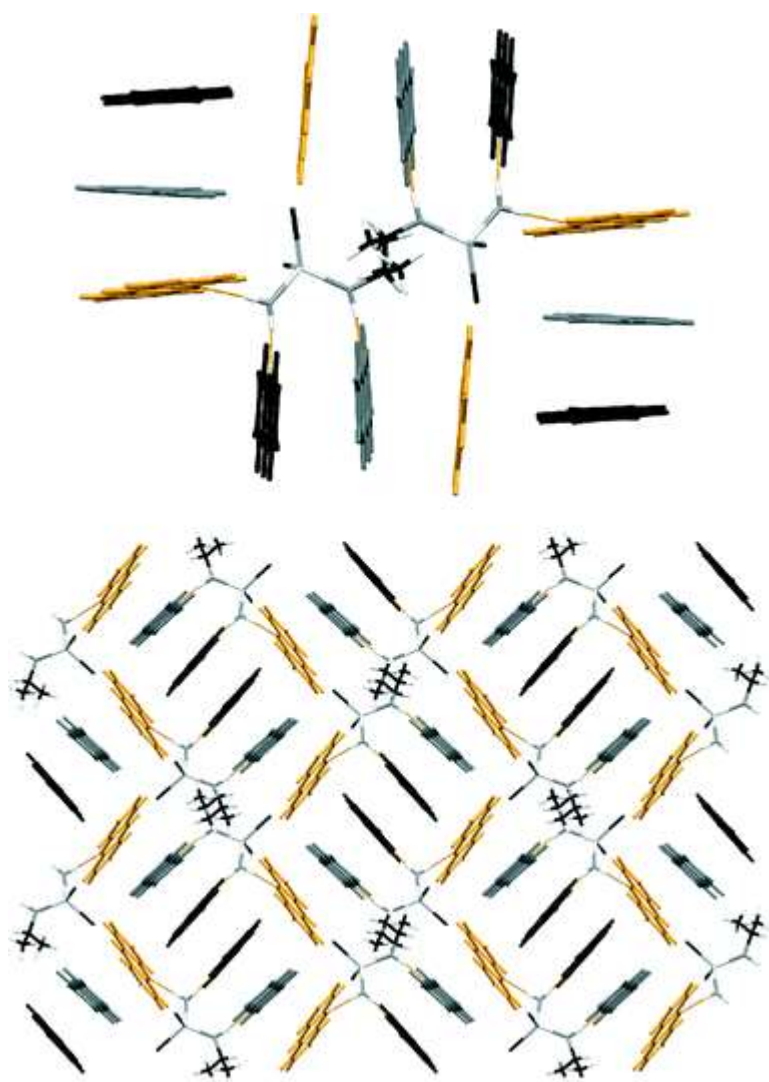
14

**Fig. 30** Non-covalent interactions in compound **14**, with the dotted orange lines indicating short contacts as per default definition given in Mercury.<sup>20</sup> Acridine molecules C, D and E are coloured orange, grey and black, respectively.

In compounds **15** and **16**, hydrophobic encapsulation still holds true (Fig. 31 and 32), but only along the bc-plane, while the inorganic pseudo-chain propagates undisturbed, albeit not formally bonded, along the direction of the crystallographic a-axis. In compound **15**, the



stacking arrangement of the organic acridine residues, although further apart, with centroid-to-centroid distances of 4.054(2) Å and 3.841(3) Å between CD and DE, respectively, follows the same CDEEDC stacking sequence as that in compound **14**. The angles between the mean planes through the CD and DE units are 8.76° and 6.74°, respectively, with relative in-plane rotations of -151.59° and -6.87°. The perpendicular slippage distance between repeating CDE units (3.132 Å) is larger than the corresponding value of 1.672 Å observed in **14**. This is also true for the corresponding edge-to-face or T-shaped arrangement between moieties C and E, with the much larger C(33)-H(33)···Cg(N1) distance of 3.27 Å and a concomitant smaller puckering amplitude of 0.040(5) Å for ring C. In compound **16**, the stacking arrangement of the organic acridine residues is more compact than that observed in **15**, with the corresponding distances comparable to those observed in **14** with centroid-to-centroid distances of 3.6078(10) Å and 3.8578(11) Å between CD and DE units, respectively. The CDEEDC ring stacking sequence holds in structure **16**, although the perpendicular slippage distance between the CDE units is larger than the corresponding distances in both **14** and **15**, at 3.639 Å. The angles between the mean planes through the CD and the DE units are 3.76° and 5.69°, respectively, with relative in-plane rotations of -137.78° and -12.32°. The edge-to-face interaction distance between moieties C and E is the smallest when comparing structures **14** to **16**, with a C-H···Cg(N1) distance of 2.76 Å, but since the arranged ring systems are not in full contact, as was the case in **14**, but shifted relative to each other with only two six-membered rings per molecule in contact with the adjacent aromatic system, the interaction does not have such a large effect on ring puckering as was the case in **14**. The total ring puckering amplitude of C is 0.0460(19) Å in structure **16**.



15

**Fig. 31** Hydrophobic encapsulation of the dimeric associate formed by the inorganic units in **15** (top).  $2 \times 2 \times 2$  packing arrangement of **15** as viewed down the crystallographic b-axis (bottom). Acridine molecules C, D and E are coloured orange, grey and black, respectively.

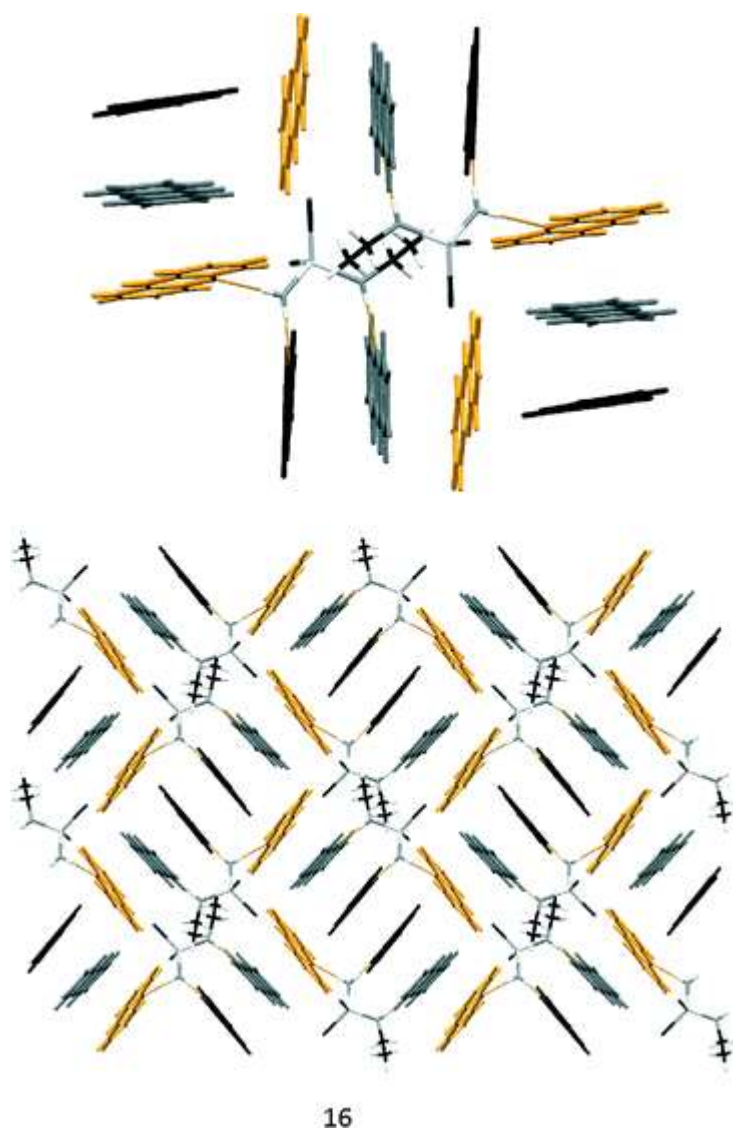


**Fig. 32** Hydrophobic encapsulation of the dimeric associate formed by the inorganic units in **16** (top).  $2 \times 2 \times 2$  packing arrangement of **16** as viewed down the crystallographic b-axis (bottom), with the acridine molecules C, D and E coloured orange, grey and black, respectively.

## Discussion

In this study, the reactant stoichiometry used experimentally and the product stoichiometry observed in the solid state do not necessarily correspond to each other. The ionic compounds, structures **1** to **10**, all contain a tetrahalometallate inorganic moiety that bears a formal charge of  $2^-$ , as well as protonated organic moieties to balance the charge. The product stoichiometry is thus driven by the overall charge balance, resulting in a  $L : MX_2$  product ratio of  $2 : 1$ , although all these compounds were synthesised with a stoichiometry of  $1 : 1$ . In the ionic compound **11**, the inorganic anion comprises a  $[Zn(OH_2)Br_3]^-$  unit, in contrast to the expected  $[ZnBr_4]^{2-}$  unit as observed in compound **7**. The reason seems to be steric in nature. In compound **7**, two of the four Zn–Br bonds of the inorganic unit engage in charge-assisted hydrogen bonding interactions, resulting in slight elongation of these two Zn–Br distances. This creates slightly more space in the tetrahedral coordination sphere of the specific  $Zn^{2+}$  cation in compound **7**. In compound **11**, none of the Zn–Br bonds engage in hydrogen bonding of the charge-assisted type and therefore no extra space is created in the  $Zn^{2+}$

coordination sphere, resulting in the coordination sphere being unable to accommodate four bromido ligands, and a  $[\text{Zn}(\text{OH}_2)\text{Br}_3]^-$  inorganic unit is formed instead.

It is interesting to note the number of water molecules included in the asymmetric unit of the ionic compounds **1** to **9**, recognising that water was present in all the crystallisations. Compounds **1** to **3**, the  $\text{Cd}^{2+}$  and  $\text{Hg}^{2+}$  compounds with phenazinium as the organic counter cation, all contain two water molecules in their respective lattices. Compounds **4** to **5**, the  $\text{Cd}^{2+}$  and  $\text{Hg}^{2+}$  compounds with quinolinium as the organic counter cation, each contain one water molecule per asymmetric unit. Compounds **6** to **9**, which represent the  $\text{Zn}^{2+}$  and  $\text{Cd}^{2+}$  ionic compounds with acridinium as the organic counter cation, contain no water molecules. The two water molecules contained per unit cell in compounds **1** to **3**, being neutral and being able to function as both a hydrogen bond donor and acceptor, serve as the perfect gap filler. As was discussed earlier and shown in Fig. 3, the chemical nature of the phenazinium cation is such that it contains both a strong hydrogen bond donor site (N–H) as well as a weak hydrogen bond acceptor site (N). Weak hydrogen bond donors and acceptors are hydrogen-bonded to each other, while strong hydrogen bond donors and acceptors are bonded. This, together with the aromatic stacking between phenazinium cations, results in the formation of the double organic layer observed in compounds **1** to **3**. Hydrogen bonding between the double organic layer and the inorganic components therefore has to occur on the periphery of the organic layer, and gap filling water molecules are required to ensure sensible space filling. In compounds **4** and **5**, the organic components of the structures, namely quinolinium cations, are smaller compared to the phenazinium and acridinium organic cations. Packing of the quinolinium cations does not result in the formation of a double organic layer as observed in compounds **1** to **3**. Here, the smaller size and the unsymmetrical nature of the quinolinium cations result in less effective space filling and water molecules are incorporated as spacer molecules. Compounds **6** to **9** contain no water molecules. Upon consideration of the respective organic layers, which comprise stacked acridinium cations, the hydrogen bond donor sites are spaced in such a way that no spacer/gap filling is required and therefore no water molecules are incorporated.

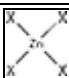


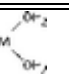
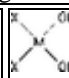
In the case of the neutral compounds **12** to **16**, water molecules are once again incorporated in the phenazine-containing compounds **12** and **13**, but not in the acridine-containing structures, compounds **14** to **16**. Association of the organic components in the respective compounds is, however, very different from that observed in the ionic compounds and the packing is no longer layered. Replacement of two halido ligands on the tetrahedral anion results in a structure type in which the inorganic dimer is encapsulated by organic moieties. In compounds **12** and **13**, each asymmetric unit contains two neutral phenazine molecules and one water molecule in addition to the neutral inorganic moiety. Each phenazine molecule, therefore, has two hydrogen bonding acceptor sites. Association of organic moieties can therefore no longer occur via sideways hydrogen bonding, as was the case in compounds **1** to **3**, but only via aromatic interactions and they can thus be described as organic portions in which the cations display the same orientation. The size of the organic phenazine molecules, together with space filling requirements, forces the organic molecules that comprise adjacent portions to be at an angle to each other. The inorganic moiety can fit into the V-space created by adjacent organic portions. A small space is, however, left vacant and is occupied by a water molecule. The neutral acridine-containing compounds **14** to **16** contain three acridine molecules, together with the respective inorganic component per unit cell. Here, complete hydrophobic encapsulation of the inorganic moieties is observed. It can thus be concluded that the product stoichiometry of compounds **12** to **16** is directed by space filling requirements and does therefore not reflect the reactant stoichiometry.

Another interesting aspect is the incorporation of aqua ligands into the coordination sphere of the metal ion in the structures of the coordination compounds **12** to **16**. In compounds **12** to **14**, the tetrahedral coordination sphere of the respective  $Zn^{2+}$  centres is coordinated, in addition to two halido ligands, by two aqua ligands each. This is in stark contrast to Bowmaker's adducts,<sup>1</sup> as well as the other adduct-type compounds listed in Table 1, in which organic N-donor ligands filled these sites. This observation can be attributed to the bulk of the organic ligands employed in the current study. There is simply no space in the  $Zn^{2+}$  coordination sphere to accommodate two of the organic N-donor ligands under investigation, while maintaining the preferred tetrahedral geometry, and aqua ligands coordinate instead. The size restriction imposed by the  $Zn^{2+}$  coordination sphere on the ligating molecules is again brought forth upon consideration of compounds **15** and **16**, as was discussed in the preceding text. Here, the inorganic moieties each comprise a  $Zn^{2+}$  cation coordinated by two large iodido ligands, one aqua ligand and one O-donor solvent molecule. One of the aqua ligands, as was seen in compounds **12** to **14**, is replaced by an O-donor solvent molecule, in order to free up space in the respective  $Zn^{2+}$  coordination spheres.

In summary, upon consideration of the neutral compounds **12** to **16**, no acid was present during crystallisation, hence protonation of the organic species and the formation of a  $[MX_4]^{2-}$  anion are not possible. One expects that neutral, tetrahedral coordination compounds of the formula  $MX_2L_2$  would be the reaction products, by analogy to Bowmaker's study.<sup>1</sup> However, the size of the organic ligands considered in the current study precludes this from occurring, due to the steric strain which would be present in such a tetrahedral complex, since  $Zn^{2+}$  prefers a tetrahedral coordination geometry in the absence of chlorine as a bridging ligand with 3,5-dihalogen N-donor pyridine ligands coordinated in the apical positions, in which case the formation of a halide-bridged polymer formed by edge-sharing between adjacent octahedra, as reported by Englert,<sup>26</sup> is observed. The only alternative is for the available solvent molecules to coordinate to the  $ZnX_2$  unit to afford the  $Zn^{2+}$  cation its preferred tetrahedral geometry. The coordinated solvent molecules are either two aqua ligands or one aqua ligand and one other solvent molecule. In the case of structures **12** and **13**, an isolated water molecule is also incorporated into the structure; however, this is not the case in structures **14** to **16**, in which three, instead of two, neutral organic molecules comprise the respective asymmetric units. The different structural types, therefore, seem to be dictated by the different chemical characteristics of the phenazine and acridine organic molecules.

To highlight the uniqueness of these compounds, Table 8 presents the statistics of CSD<sup>3</sup> (version 5.35, May 2015 update) search results in which the first row gives a schematic representation of the CSD search fragment used in the respective searches and the second row lists the number of resulting hits. M represents any transition metal.

**Table 8** CSD<sup>3</sup> search fragments and resulting hits. M = transition metal, excluding  $Zn^{2+}$

Search fragment					
# hits	778	$Zn^{2+} = 20$	$Zn^{2+} = 8$	$Zn^{2+} = 0$	$Zn^{2+} = 0$
		$M^{2+} = 12$	$M^{2+} = 11$	$M^{2+} = 0$	$M^{2+} = 0$

**Table 9** Hydrogen bonding parameters for compounds **1–16** [Å and °]

	D–H...A	d(D–H) (Å)	d(H...A) (Å)	d(D...A) (Å)	∠(DHA) (°)	Symmetry operator
<b>1</b>	N(1)– H(1N1)...O(1)	0.81(5)	1.91(5)	2.709(8)	174(5)	# <sup>1</sup> –x + 1, –y, –z # <sup>2</sup> –x, –y, –z + 1 # <sup>3</sup> –x, y – 1/2, –z + 1/2
	O(2)– H(1O2)...Cl(4)	1.062(6)	2.1040(18)	3.165(6)	177.4(4)	
	N(3)– H(1N3)...Cl(2)	0.86(5)	2.26(5)	3.110(6)	174(4)	
	O(2)– H(2O2)...Cl(3) <sup>#2</sup>	0.682(7)	2.5574(16)	3.210(7)	161.2(4)	
	O(1)– H(1O1)...Cl(3) <sup>#3</sup>	0.86(12)	2.57(12)	3.364(7)	154(11)	
	O(1)– H(2O1)...O(2)	0.76(5)	1.96(6)	2.712(8)	174(6)	
	C(5)–H(5)...N(4) <sup>#1</sup>	0.93	2.69	3.614(8)	174.1	
	C(17)– H(17)...N(2) <sup>#1</sup>	0.93	2.63	3.540(8)	166.5	
	C(2)–H(2)...Cl(4)	0.93	2.88	3.592(6)	134.8	
	C(14)– H(14)...Cl(1)	0.93	2.79	3.596(6)	145.1	
<b>2</b>	N(1)– H(1N1)...O(1)	1.1(3)	1.6(3)	2.69(2)	179(24)	# <sup>1</sup> x, –y + 1/2, z – 1/2 # <sup>2</sup> –x, –y + 1, –z + 1 # <sup>3</sup> x, –y + 3/2, z – 1/2 # <sup>4</sup> –x + 1, y + 1/2, –z + 1/2 # <sup>5</sup> –x + 1, –y + 1, –z + 1
	O(2)– H(1O2)...Br(4) <sup>#3</sup>	0.70(7)	2.94(12)	3.292(19)	114(8)	
	N(3)– H(1N3)...Br(2) <sup>#1</sup>	0.771(15)	2.496(2)	3.242(15)	163.3(11)	
	O(2)– H(2O2)...Br(3) <sup>#4</sup>	1.1(3)	2.2(3)	3.326(19)	176(20)	
	O(1)– H(1O1)...Br(3) <sup>#5</sup>	0.858(16)	2.798(2)	3.424(16)	131.1(11)	
	O(1)– H(2O1)...O(2)	0.855(16)	2.248(18)	2.68(2)	111.3(12)	
	C(5)–H(5)...N(2) <sup>#2</sup>	0.93	2.59	3.49(2)	164.7	
	C(17)– H(17)...N(4) <sup>#2</sup>	0.93	2.65	3.58(3)	174.1	
	C(2)– H(2)...Br(1) <sup>#1</sup>	0.93	2.91	3.67(2)	140.1	
	C(14)– H(14)...Br(4) <sup>#3</sup>	0.93	2.99	3.707(19)	135.0	
C(11)– H(11)...Br(3)	0.93	3.12	3.635(19)	116.4		
<b>3</b>	N(1)– H(1N1)...O(1)	1.106(8)	1.670(9)	2.721(12)	156.7(6)	# <sup>1</sup> x – 1, y, z + 1 # <sup>2</sup> x + 1, y, z – 1 # <sup>3</sup> –x + 2, –y + 1, –z + 1 # <sup>4</sup> x, –y + 3/2, z – 1/2
	O(2)– H(1O2)...Br(3)	0.829(14)	2.6424(11)	3.325(12)	140.7(11)	
	N(3)–	1.051(8)	2.3876(10)	3.242(8)	137.6(5)	

	D-H...A	d(D-H) (Å)	d(H...A) (Å)	d(D...A) (Å)	∠(DHA) (°)	Symmetry operator
	H(1N3)···Br(2)					
	O(1)– H(1O1)···Br(3) <sup>#4</sup>	0.868(12)	2.6856(13)	3.482(12)	153.0(7)	
	O(1)– H(2O1)···O(2)	0.888(11)	1.772(12)	2.653(16)	170.6(8)	
	C(11)– H(11)···Br(4) <sup>#3</sup>	0.93	2.99	3.737(12)	138.3	
	C(20)– H(20)···N(2) <sup>#1</sup>	0.93	2.63	3.550(14)	168.8	
	C(8)–H(8)···N(4) <sup>#2</sup>	0.93	2.68	3.604(14)	173.6	
	C(23)– H(23)···Br(1)	0.93	2.92	3.721(11)	144.4	
<b>4</b>	C(2)– H(2)···Br(2) <sup>#1</sup>	0.93	2.93	3.819(5)	160.6	<sup>#1</sup> –x – 1/2, y – 1/2, –z + 1/2 <sup>#2</sup> –x, y, –z + 1/2
	C(9)–H(9)···O(1) <sup>#2</sup>	0.93	2.54	3.352(7)	146.0	
	N(1)– H(1N1)···O(1)	0.79(6)	2.01(6)	2.779(6)	165(6)	
	O(1)– H(1O1)···Br(1) <sup>#1</sup>	0.73(8)	2.95(9)	3.621(7)	154(9)	
	O(1)– H(2O1)···Br(1)	0.79(11)	2.60(11)	3.369(7)	166(12)	
<b>5</b>	C(2)– H(2)···Cl(2) <sup>#1</sup>	0.93	2.89	3.765(2)	157.9	
	C(9)–H(9)···O(1) <sup>#2</sup>	0.93	2.58	3.360(2)	141.6	
	N(1)– H(1N1)···O(1)	0.91(3)	1.91(3)	2.816(2)	177(3)	
	O(1)– H(1O1)···Cl(1) <sup>#1</sup>	0.81(4)	2.86(4)	3.5794(19)	150(3)	
	O(1)– H(1O1)···Cl(2) <sup>#1</sup>	0.81(4)	3.05(4)	3.5352(17)	121(3)	
	O(1)– H(2O1)···Cl(1)	0.78(3)	2.54(3)	3.289(2)	163(3)	
<b>6</b>	N(1)– H(1N1)···Cl(1) <sup>#1</sup>	1.26(15)	2.15(15)	3.343(12)	157(11)	<sup>#1</sup> –x, y, –z + 1/2 <sup>#2</sup> –x, –y, –z
<b>7</b>	N(1)– H(1N1)···Br(2)	0.73	2.65	3.357(15)	163.6	
	C(2)–H(2)···Br(2)	0.93	3.11	3.84(2)	137.1	
	C(12)– H(12)···Br(2) <sup>#1</sup>	0.93	3.10	3.99(2)	160.4	
<b>8</b>	N(1)– H(1N1)···Cl(1)	1.003(9)	2.254(3)	3.189(10)	154.6(6)	

	D-H...A	d(D-H) (Å)	d(H...A) (Å)	d(D...A) (Å)	∠(DHA) (°)	Symmetry operator
9	N(1)- H(1N1)...Br(4)	0.88(4)	2.58(4)	3.352(3)	148(3)	
	N(2)- H(1N2)...Br(2) <sup>#2</sup>	1.05(4)	2.46(4)	3.476(3)	164(3)	
10	C(8)- H(8)...Cl(2) <sup>#1</sup>	0.93	2.94	3.676(4)	137.0	<sup>#1</sup> x - 1/2, -y + 3/2, z - 1/2
	N(1)- H(1N1)...Cl(1)	0.78(5)	2.36(5)	3.128(4)	167(5)	
	N(2)- H(1N2)...Cl(2) <sup>#1</sup>	0.77(4)	2.41(4)	3.177(3)	173(4)	
11	C(8)- H(8)...Br(3) <sup>#3</sup>	0.93	2.98	3.8492(15)	155.7	<sup>#1</sup> -x, -y + 1, -z <sup>#2</sup> -x + 1, -y + 1, -z <sup>#3</sup> -x, -y, -z + 1 <sup>#4</sup> x + 1, y, z <sup>#5</sup> x - 1, y, z
	C(17)- H(17)...Br(1)	0.93	3.11	4.0037(15)	161.9	
	C(25)- H(25A)...Br(3) <sup>#4</sup>	0.97	2.97	3.8152(15)	146.2	
	N(1)- H(1N1)...O(3)	1.01(3)	1.69(3)	2.6897(15)	172(2)	
	O(1)- H(1O1)...N(3)	0.80(3)	1.96(3)	2.7448(15)	169(3)	
	O(2)- H(1O2)...Br(1) <sup>#5</sup>	0.85(3)	2.48(3)	3.2954(13)	163(2)	
	O(3)- H(1O3)...Br(2)	0.82(3)	2.77(3)	3.2401(11)	118(3)	
	O(3)- H(1O3)...O(2) <sup>#4</sup>	0.82(3)	2.17(3)	2.8934(16)	146(3)	
	O(1)- H(2O1)...O(2)	0.80(3)	1.91(3)	2.7118(16)	172(2)	
	O(2)- H(2O2)...N(4) <sup>#5</sup>	0.59(3)	2.31(3)	2.8663(16)	158(4)	
12	O(1)-H(21)...O(3)	0.950(9)	1.824(8)	2.773(12)	176.5(9)	x + 1, y, z
	O(2)-H(23)...O(3)	0.951(9)	1.824(8)	2.775(12)	179.8(8)	
	O(2)-H(24)...N(2)	0.950(9)	1.814(9)	2.765(12)	179.8(8)	-x + 1, -y + 1, -z + 1
	O(3)-H(20)...N(3)	0.951(7)	1.935(9)	2.886(11)	179.8(6)	x - 1, -y + 1/2, z - 1/2
	O(3)-H(19)...N(1)	0.949(8)	1.955(9)	2.904(12)	179.8(6)	x - 1, -y + 1/2, z - 1/2
	O(1)-H(22)...N(4)	0.951(9)	1.777(9)	2.727(12)	179.7(10)	-x + 1, -y, -z + 1
	C(12)-H(5)...Cl(1)	0.95	2.91	3.585(12)	128.7	x + 1, -y + 1/2, z + 1/2
	C(17)- H(12)...Cl(1)	0.95	2.97	3.833(13)	151.9	-x + 1, -y, -z + 1
	C(24)- H(13)...Cl(2)	0.95	2.83	3.599(11)	138.9	x, -y + 1/2, z + 1/2



	D–H…A	d(D–H) (Å)	d(H…A) (Å)	d(D…A) (Å)	∠(DHA) (°)	Symmetry operator
13	C(8)–H(8)…Br(2)	0.93	3.03	3.670(7)	127.7	-x + 1, y - 1/2, -z + 1/2
	C(14)– H(14)…Br(2)	0.93	3.06	3.887(7)	149.2	
	C(20)– H(20)…Br(1)	0.93	2.92	3.677(7)	138.9	-x, y + 1/2, -z + 1/2
	O(1)– H(1O1)…N(3)	0.80(12)	1.94(12)	2.731(8)	170(11)	
	O(2)– H(1O2)…O(3)	0.79(10)	2.01(10)	2.782(8)	165(9)	-x + 1, y - 1/2, -z + 1/2
	O(3)– H(1O3)…N(4)	0.90(10)	2.01(11)	2.890(7)	163(9)	
	O(1)– H(2O1)…O(3)	0.81(9)	1.99(9)	2.786(8)	168(8)	-x, y - 1/2, -z + 1/2
	O(2)– H(2O2)…N(1)	0.81(12)	1.96(12)	2.753(8)	168(11)	
	O(3)– H(2O3)…N(2)	0.66(11)	2.29(12)	2.931(8)	168(13)	x, y + 1, z
14	C(2)–H(2)…Br(2)	0.95	3.08	3.914(4)	147.2	-x + 3/2, y - 1/2, -z - 1/2
	C(15)– H(15)…Br(1)	0.95	3.11	3.973(4)	152.0	
	O(1)– H(2O1)…N(1)	0.77(4)	1.92(4)	2.672(4)	168(4)	-x + 3/2, y + 1/2, -z - 1/2
	O(1)– H(1O1)…N(3)	0.75(5)	1.96(5)	2.699(4)	172(5)	
	O(2)– H(1O2)…N(2)	0.70(6)	1.97(6)	2.658(5)	167(7)	
	O(2)– H(2O2)…Br(1)	0.80(5)	2.44(5)	3.235(3)	174(4)	-x + 2, -y, -z
15	C(42)– H(42B)…I(1)	0.96	3.30	4.082(8)	140.3	
	O(1)– H(1O1)…N(1)	0.912(2)	1.787(3)	2.689(4)	169.21(19)	
	O(2)– H(1O2)…N(2)	1.026(3)	1.647(3)	2.661(4)	168.92(19)	
	O(1)– H(2O1)…N(3)	0.919(3)	1.836(3)	2.752(4)	174.5(2)	
16	C(15)– H(15C)…I(1)	0.98	3.33	4.096(3)	136.6	
	O(1)– H(1O1)…N(1)	0.85(3)	1.79(3)	2.640(2)	177(3)	
	O(2)– H(1O2)…N(2)	0.80(3)	1.86(3)	2.651(2)	170(3)	
	O(2)– H(2O2)…N(3)	0.80(3)	1.93(3)	2.724(2)	175(3)	

**Table 10** Ring interaction parameters in **1–16**. Cg(Z) is the centroid of the six-membered heterocyclic ring with Cg–Cg as the distance between the ring centroids.  $\alpha$  is the dihedral angle between planes I and J,  $\beta$  is the angle between the Cg(I)–Cg(J) vector and the normal to plane I, and  $\gamma$  is the angle between the Cg(I)–Cg(J) vector and the normal to plane J ( $^\circ$ ). Cg(I)<sub>p</sub> is the perpendicular distance of Cg(I) on ring J and Cg(J)<sub>p</sub> is the perpendicular distance of Cg(J) on ring I ( $\text{Å}$ ). Slippage is the distance between Cg(I) and the perpendicular projection of Cg(J) on ring I ( $\text{Å}$ )

	Cg(I)–Cg(J)	Cg–Cg ( $\text{Å}$ )	$\alpha$ ( $^\circ$ )	$\beta$ ( $^\circ$ )	$\gamma$ ( $^\circ$ )	Cg(I) <sub>p</sub> ( $\text{Å}$ )	Cg(J) <sub>p</sub> ( $\text{Å}$ )	Symmetry operator
<b>1</b>	Cg(N1)–Cg(N3) <sup>#</sup>	3.950(3)	4.6(2)	31.4	28.7	–3.463(2)	–3.372(2)	#1 – x, –y, 1 – z
	Cg(N1)–Cg(N3) <sup>#</sup>	3.917(10)	4.4(8)	31.7	29.6	–3.405(7)	–3.332(7)	
	Cg(N1)–Cg(N3)	3.964(6)	4.6(5)	31.2	28.5	3.484(4)	–3.392(4)	
<hr/>								
<b>4</b>	Cg(N1)–Cg(N1) <sup>#</sup>	3.943(3)	0	26.1	26.1	–3.5421(19)	–3.542(2)	1.733
<b>5</b>	Cg(N1)–Cg(N1) <sup>#</sup>	3.8115(9)	0	25.6	25.6	–3.4372(6)	–3.4372(6)	1.647
<hr/>								
<b>6</b>	Cg(N1)–Cg(N1) <sup>#1</sup>	4.057(10)	0	30.2	30.2	3.507(6)	3.507(6)	2.040
	Cg(N1)–Cg(N1) <sup>#2</sup>	4.350(10)	0	35.7	35.7	–3.532(6)	–3.532(6)	2.539
<hr/>								
<b>7</b>	Cg(N1)–Cg(N1) <sup>#1</sup>	3.973(10)	0	28.9	28.9	–3.478(7)	–3.479(7)	1.921
	Cg(N1)–Cg(N1) <sup>#2</sup>	4.380(10)	0	37.8	37.8	3.461(7)	3.461(7)	2.684
<hr/>								
<b>8</b>	Cg(N1)–Cg(N1) <sup>#1</sup>	3.919(7)	0	29.6	29.6	3.409(5)	3.408(5)	1.933
	Cg(N1)–Cg(N1) <sup>#2</sup>	4.312(7)	0	36.5	36.5	–3.465(5)	–3.466(5)	2.566
<hr/>								
<b>9</b>	Cg(N1)–Cg(N1) <sup>#3</sup>	3.8353(19)	0	21.9	21.9	–3.5597(13)	–3.5596(13)	1.428
	Cg(N2)–Cg(N2) <sup>#1</sup>	4.237(2)	0	36.5	36.5	–3.4062(15)	–3.4062(15)	2.519
	Cg(N2)–Cg(N2) <sup>#4</sup>	5.635(2)	0	55.3	55.3	3.2097(15)	3.2097(15)	4.632
<hr/>								
<b>10</b>	Cg(N1)–Cg(N1) <sup>#1</sup>	3.254(2)	0	9.5	9.5	3.209(15)	3.209(15)	0.535
	Cg(N1)–Cg(N2) <sup>#2</sup>	3.582(2)	2.86(17)	18.1	17.9	3.409(15)	–3.404(14)	
<hr/>								
<b>11</b>	Cg(N1)–Cg(N1) <sup>#1</sup>	3.7242(8)	0	23.0	23.0	3.4287(6)	3.4287(6)	1.454
	Cg(N3)–Cg(N4) <sup>#2</sup>	3.8760(8)	1.47(7)	25.1	25.9	3.4859(6)	–3.5102(6)	
<hr/>								
<b>14</b>	Cg(N1)–Cg(N2)	3.539(2)	3.10(16)	21.5	19.2	3.3426(13)	–3.2920(15)	
	Cg(N2)–Cg(N3)	3.704(2)	8.39(18)	21.1	24.4	3.3729(15)	–3.4556(16)	
	Cg(N3)–Cg(N3) <sup>#</sup>	3.906(2)	0	25.3	25.3	–3.5302(15)	–3.5301(15)	1.672
<hr/>								
<b>15</b>	Cg(N1)–Cg(N2)	3.841(3)	7.0(2)	27.8	24.0	3.5104(16)	–3.3966(17)	
	Cg(N2)–Cg(N3)	4.054(2)	9.2(2)	30.3	23.8	3.7082(17)	–3.5010(16)	
	Cg(N3)–Cg(N3) <sup>#</sup>	4.693(3)	0	41.9	41.9	3.4955(16)	3.4955(16)	3.132
<hr/>								
<b>16</b>	Cg(N1)–Cg(N2)	3.6078(10)	4.31(8)	22.0	18.6	3.4199(7)	–3.3448(7)	
	Cg(N2)–Cg(N3)	3.8578(11)	3.21(9)	26.0	26.6	3.4494(8)	–3.4674(8)	
	Cg(N3)–Cg(N3) <sup>#</sup>	4.9890(11)	0	46.8	46.8	3.4123(7)	3.4124(7)	3.639

**Table 11** Anion...Cg (aromatic) interaction parameters in compounds **1–3** and **11**. Cg(J) is the center of gravity of ring J (atom number), with X-Perp as the perpendicular distance of H to ring plane J.  $\gamma$  represents the angle between the Cg–H vector and the ring normal. Anion...Cg < 4.0 Å and  $\gamma$  < 30.0°

	Y–X	Cg(J)	X...Cg (Å)	X-Perp (Å)	$\gamma$ (°)	Y–X...Cg (°)	Y...Cg (Å)	Symmetry operator
<b>1</b>	Hg(1)–Cl(1)	Cg(N3) <sup>#</sup>	3.298(3)	3.212	13.12	118.43(7)	4.953(2)	x, 1/2 – y, 1/2 + z
	Hg(1)–Cl(1)	Cg(C19) <sup>#</sup>	3.587(3)	3.228	25.83	83.01(6)	4.088(2)	x, 1/2 – y, 1/2 + z
	Hg(1)–Cl(4)	Cg(N1) <sup>#</sup>	3.321(3)	3.306	5.44	169.64(8)	5.799(2)	x, –1 + y, z
<b>2</b>	Hg(1)–Br(1)	Cg(N3) <sup>#</sup>	3.333(7)	3.279	10.31	114.17(15)	4.974(7)	x, 1/2 – y, –1/2 + z
	Hg(1)–Br(1)	Cg(C7) <sup>#</sup>	3.716(8)	3.303	27.29	80.23(14)	4.145(8)	x, 1/2 – y, –1/2 + z
	Hg(1)–Br(4)	Cg(N1) <sup>#</sup>	3.300(7)	3.288	4.78	169.19(15)	5.883(7)	1 – x, –1/2 + y, 1/2 – z
<b>3</b>	Cd(1)–Br(1)	Cg(N3) <sup>#</sup>	3.409(4)	–3.330	12.31	116.54(8)	5.108(4)	x, 1/2 – y, –1/2 + z
	Cd(1)–Br(1)	Cg(C19) <sup>#</sup>	3.711(5)	–3.345	25.64	83.11(8)	4.255(5)	x, 1/2 – y, –1/2 + z
	Cd(1)–Br(4)	Cg(N1) <sup>#</sup>	3.366(4)	3.354	4.97	169.53(9)	5.928(4)	x, 3/2 – y, 1/2 + z
<b>11</b>	Zn(4)–Br(3)	Cg(N3) <sup>#</sup>	3.8266(6)	–3.588	20.34	92.87(1)	4.5989(6)	
	Zn(4)–Br(3)	Cg(C1) <sup>#</sup>	3.7497(7)	–3.583	17.13	92.89(1)	4.5339(7)	

**Table 12** X–H...Cg (aromatic ring) interaction parameters for compounds **14** and **16**. Cg(J) is the center of gravity of ring J (atom number), with H-Perp as the perpendicular distance of H to ring plane J.  $\gamma$  represents the angle between the Cg–H vector and the ring normal. Anion...Cg < 4.0 Å and  $\gamma$  < 30.0°

	X...H	Cg(J)	H...Cg (Å)	H-Perp (Å)	$\gamma$ (°)	X–H...Cg (°)	X...Cg (Å)	$\angle$ (X–H–J) (°)	Symmetry operator
<b>14</b>	C(33)–H(33)	Cg(N1)	2.88	2.76	16.70	158	3.776(4)	81	1/2 + x, 1/2 – y, 1/2 + z
<b>16</b>	C(20)–H(20)	Cg(N1)	2.76	–2.70	11.94	159	3.658(2)	79	1/2 + x, 1/2 – y, –1/2 + z

From the CSD<sup>3</sup> search results, it can be seen that structures **15** and **16** are the first reported structures to contain tetrahedral, isolated [Zn(OH<sub>2</sub>)X<sub>2</sub>(O<sup>–</sup>prop)] and [Zn(OH<sub>2</sub>)X<sub>2</sub>(O–EtOH)] inorganic units in a crystal structure, for any metal ion M<sup>2+</sup> and any halogen X. The formation of these unique inorganic units can be attributed to the steric bulk of the organic molecules that prevents the formation of the expected coordination compounds, and this implies that the organic molecule has a templating effect on the inorganic species formed.

## Conclusion

It was found that the formation of an [MX<sub>4</sub>]<sup>2–</sup> anion and protonation of the benzopyridine or -pyrazine molecule typically occur in the presence of an acid HX, which dictates the structural stoichiometry, and result in strong hydrogen bonding interactions in the structure. In the case of the neutral compounds, the larger molecules acridine and phenazine do not coordinate to the MX<sub>2</sub> unit due to their bulkiness, and inorganic moieties of the type MX<sub>x</sub>solvent<sub>4–x</sub> are formed instead, with the neutral organic molecules incorporated into the structure. The presence of water molecules in certain structures can be attributed to their ability to act as space filling molecules.

## Experimental

### Chemicals and reagents

All chemicals were used as-purchased without further purification: HgCl<sub>2</sub> (98%, Fluka), HgBr<sub>2</sub> (98%, Sigma Aldrich), HgI<sub>2</sub> (99%, Riedel de Haen), CdCl<sub>2</sub>·2.5H<sub>2</sub>O (99%, Riedel de Haen), CdBr<sub>2</sub>·4H<sub>2</sub>O (99%, Riedel de Haen), phenazine (98%, Sigma Aldrich), quinoxaline (98%, Sigma Aldrich), ethanol (99.5%, Merck), methanol (99%, Merck), isopropanol (Sigma Aldrich), acetonitrile (99.9%, Merck) and tetrahydrofuran (99.9%, Merck).

All reactions were carried out in a stoichiometric L : MX<sub>2</sub> ratio of 1 : 1. Good quality single crystals were harvested from the reaction vessels, with no attempt made to maximise yields from crystallisations. Matching of the experimental PXRD patterns with the PXRD patterns simulated from SXR data, for all compounds, is given in the ESI. † Microanalyses of the compounds, of which enough material could be obtained, were performed using a Flash 2000 CHNS-O analyzer.

Synthesis of [phe-H]<sub>2</sub>[HgCl<sub>4</sub>]·2H<sub>2</sub>O (**1**). 1.2 ml of a 0.50 M HCl solution was added to a stirred solution of phenazine (0.55 mmol, 0.102 g) in 6 ml of ethanol. The solution was brought to boiling for five minutes, after which the temperature was reduced to allow the addition of a solution of HgCl<sub>2</sub> (0.55 mmol, 0.154 g) dissolved in 2 ml of ethanol. The resulting solution was brought to boiling. Boiling was continued until the volume of the reaction mixture was reduced by ca. 1 ml, after which it was left to cool to room temperature (ca. 23 °C). The reaction vessel was covered with perforated Parafilm and left at room temperature for crystallisation. A batch of yellow crystals of **1** were harvested upon formation.

Synthesis of [phe-H]<sub>2</sub>[HgBr<sub>4</sub>]·2H<sub>2</sub>O (**2**). 1.5 ml of a 0.50 M HBr solution was added to a stirred solution of phenazine (0.55 mmol, 0.106 g) in 6 ml of ethanol. The solution was brought to boiling for five minutes, after which the temperature was reduced to allow the addition of a solution of HgBr<sub>2</sub> (0.55 mmol, 0.214 g) dissolved in 2 ml of ethanol. The resulting solution was brought to boiling. Boiling was continued until the volume of the reaction mixture was reduced by ca. 1 ml, after which it was left to cool to room temperature (ca. 23 °C). The reaction vessel was covered with perforated Parafilm and left at room temperature for crystallisation. A batch of yellow-brown crystals of **2** were harvested upon formation.

Synthesis of [phe-H]<sub>2</sub>[CdBr<sub>4</sub>]·2H<sub>2</sub>O (**3**). 1.3 ml of a 0.50 M HBr solution was added to a stirred solution of phenazine (0.55 mmol, 0.113 g) in 6 ml of ethanol. The solution was brought to boiling for five minutes, after which the temperature was reduced to allow the addition of a solution of CdBr<sub>2</sub>·4H<sub>2</sub>O (0.55 mmol, 0.198 g) dissolved in 2 ml of EtOH. The resulting solution was brought to boiling. Boiling was continued until the volume of the reaction mixture was reduced by ca. 1 ml, after which it was left to cool to room temperature (ca. 23 °C). The reaction vessel was covered with perforated Parafilm and left at room temperature for crystallisation. A batch of light yellow plate-like crystals of **3** were harvested upon formation. Found for **3**: C, 34.74; H, 2.78; N, 6.92%; calcd. for C<sub>24</sub>H<sub>22</sub>N<sub>4</sub>O<sub>2</sub>CdBr<sub>4</sub>: C, 34.71; H, 2.67; N, 6.75%.

Synthesis of [quin-H]<sub>2</sub>[CdBr<sub>4</sub>]·H<sub>2</sub>O (**4**). 1.8 ml of a 0.50 M HBr solution was added to a stirred solution of quinoxaline (0.77 mmol, 0.103 g) in 6 ml of ethanol. The solution was brought to boiling for five minutes, after which the temperature was reduced to allow the addition of a solution of CdBr<sub>2</sub>·4H<sub>2</sub>O (0.77 mmol, 0.240 g) dissolved in 2 ml of ethanol. The resulting solution was brought to boiling. Boiling was continued until the volume of the

reaction mixture was reduced by ca. 1 ml, after which it was left to cool to room temperature (ca. 23 °C). The reaction vessel was covered with perforated Parafilm and left at room temperature for crystallisation. A batch of colourless, plate-like crystals of **4** were harvested upon formation. Found for **4**: C, 34.50; H, 2.60; N, 3.80%; calcd. for C<sub>18</sub>H<sub>20</sub>N<sub>2</sub>O<sub>2</sub>CdBr<sub>4</sub>: C, 29.68; H, 2.77; N, 3.85%.

Synthesis of [quin-H]<sub>2</sub>[HgCl<sub>4</sub>]·H<sub>2</sub>O (**5**). 2.0 ml of a 0.50 M HCl solution was added to a stirred solution of quinoxaline (0.77 mmol, 0.104 g) in 6 ml of methanol. The solution was brought to boiling for five minutes, after which the temperature was reduced to allow the addition of a solution of HgBr<sub>2</sub> (0.77 mmol, 0.210 g) dissolved in 2 ml of methanol. The resulting solution was brought to boiling. Boiling was continued until the volume of the reaction mixture was reduced by ca. 1 ml, after which it was left to cool to room temperature (ca. 23 °C). The reaction vessel was covered with perforated Parafilm and left at room temperature for crystallisation. A batch of flaky, colourless crystals of **5** were harvested upon formation.

Synthesis of [acr-H]<sub>2</sub>[ZnCl<sub>4</sub>] (**6**). 3.0 ml of a 0.50 M HCl solution was added to a stirred solution of acridine (0.55 mmol, 0.103 g) in 5 ml of ethanol. The solution was brought to boiling for five minutes, after which the temperature was reduced to allow the addition of a solution of ZnCl<sub>2</sub> (0.55 mmol, 0.125 g) dissolved in 2 ml of ethanol. The resulting solution was brought to boiling. Boiling was continued until the volume of the reaction mixture was reduced by ca. 1 ml, after which it was left to cool to room temperature (ca. 23 °C). The reaction vessel was covered with perforated Parafilm and left at room temperature for crystallisation. Crystals of **6** were harvested upon formation.

Synthesis of [acr-H]<sub>2</sub>[ZnBr<sub>4</sub>] (**7**). 3.0 ml of a 0.50 M HBr solution was added to a stirred solution of acridine (0.55 mmol, 0.121 g) in 5 ml of ethanol. The solution was brought to boiling for five minutes, after which the temperature was reduced to allow the addition of a solution of ZnBr<sub>2</sub> (0.55 mmol, 0.195 g) dissolved in 2 ml of ethanol. The resulting solution was brought to boiling. Boiling was continued until the volume of the reaction mixture was reduced by ca. 1 ml, after which it was left to cool to room temperature (ca. 23 °C). The reaction vessel was covered with perforated Parafilm and left at room temperature for crystallisation. A batch of light yellow crystals of **7** were harvested upon formation. Found for **7**: C, 41.37; H, 2.84; N, 3.86%; calcd. for C<sub>26</sub>H<sub>20</sub>N<sub>2</sub>ZnBr<sub>4</sub>: C, 41.89; H, 2.70; N, 3.76%.

Synthesis of [acr-H]<sub>2</sub>[CdCl<sub>4</sub>] (**8**). 1.2 ml of a 0.50 M HCl solution was added to a stirred solution of acridine (0.55 mmol, 0.094 g) in 6 ml of ethanol. The solution was brought to boiling for five minutes, after which the temperature was reduced to allow the addition of a solution of CdCl<sub>2</sub>·2.5H<sub>2</sub>O (0.55 mmol, 0.083 g) dissolved in 2 ml of ethanol. The resulting solution was brought to boiling. Boiling was continued until the volume of the reaction mixture was reduced by ca. 1 ml, after which it was left to cool to room temperature (ca. 23 °C). The reaction vessel was covered with perforated Parafilm and left at room temperature for crystallisation. A batch of orange crystals of **8** were harvested upon formation. Found for **8**: C, 50.65; H, 2.66; N, 4.48%; calcd. for C<sub>26</sub>H<sub>20</sub>N<sub>2</sub>CdCl<sub>4</sub>: C, 50.80; H, 3.28; N, 4.56%.

Synthesis of [acr-H]<sub>2</sub>[CdBr<sub>4</sub>] (**9**). 1.2 ml of a 0.50 M HBr solution was added to a stirred solution of acridine (0.55 mmol, 0.105 g) in 6 ml of ethanol. The solution was brought to boiling for five minutes, after which the temperature was reduced to allow the addition of a solution of CdBr<sub>2</sub>·4H<sub>2</sub>O (0.55 mmol, 0.136 g) dissolved in 2 ml of ethanol. The resulting solution was brought to boiling. Boiling was continued until the volume of the reaction mixture was reduced by ca. 1 ml, after which it was left to cool to room temperature (ca. 23 °C). The reaction vessel was covered with perforated Parafilm and left at room temperature for crystallisation. Crystals of **9** were harvested upon formation. Found for **9**: C, 39.49; H, 2.82; N, 3.42%; calcd. for C<sub>26</sub>H<sub>20</sub>N<sub>2</sub>CdBr<sub>4</sub>: C, 39.41; H, 2.54; N, 3.53%.

Synthesis of [phe-H]<sub>2</sub>phe[ZnCl<sub>4</sub>] (**10**). 1.2 ml of a 0.50 M HCl solution was added to a stirred solution of phenazine (0.55 mmol, 0.103 g) in 6 ml of ethanol. The solution was brought to boiling for five minutes, after which the temperature was reduced to allow the addition of a solution of ZnCl<sub>2</sub> (0.55 mmol, 0.076 g) dissolved in 2 ml of ethanol. The resulting solution was brought to boiling. Boiling was continued until the volume of the reaction mixture was reduced by ca. 1 ml, after which it was left to cool to room temperature (ca. 23 °C). The reaction vessel was covered with perforated Parafilm and left at room temperature for crystallisation. Crystals of **10** were harvested from the dark green reaction mixture upon formation.

Synthesis of [phe-H](phe)<sub>2</sub>[Zn(OH<sub>2</sub>)Br<sub>3</sub>]·EtOH·H<sub>2</sub>O (**11**). 1.2 ml of a 0.50 M HBr solution was added to a stirred solution of phenazine (0.55 mmol, 0.105 g) in 6 ml of ethanol. The solution was brought to boiling for five minutes, after which the temperature was reduced to allow the addition of a solution of ZnBr<sub>2</sub> (0.55 mmol, 0.121 g) dissolved in 2 ml of ethanol. The resulting solution was brought to boiling. Boiling was continued until the volume of the reaction mixture was reduced by ca. 1 ml, after which it was left to cool to room temperature (ca. 23 °C). The reaction vessel was covered with perforated Parafilm and left at room temperature for crystallisation. Crystals of **11** were harvested from the dark green reaction mixture upon formation.

Synthesis of (phe)<sub>2</sub>[Zn(OH<sub>2</sub>)<sub>2</sub>Cl<sub>2</sub>]·H<sub>2</sub>O (**12**). Phenazine (0.55 mmol, 0.103 g) was dissolved in 8 ml of methanol, after which a solution of ZnCl<sub>2</sub> (0.55 mmol, 0.075 g) dissolved in 2 ml of ethanol was added. The reaction vessel was left open to the atmosphere at room temperature (ca. 23 °C) for crystallisation. Green crystals of **12** were harvested upon formation.

Synthesis of (phe)<sub>2</sub>[Zn(OH<sub>2</sub>)<sub>2</sub>Br<sub>2</sub>]·H<sub>2</sub>O (**13**). Phenazine (0.55 mmol, 0.117 g) was dissolved in 8 ml of methanol, after which a solution of ZnBr<sub>2</sub> (0.55 mmol, 0.129 g) dissolved in 2 ml of ethanol was added. The reaction vessel was left open to the atmosphere at room temperature (ca. 23 °C) for crystallisation. Green crystals of **13** were harvested upon formation.

Synthesis of (acr)<sub>3</sub>[Zn(OH<sub>2</sub>)<sub>2</sub>Br<sub>2</sub>] (**14**). Acridine (0.55 mmol, 0.116 g) was dissolved in 8 ml of methanol, after which a solution of ZnBr<sub>2</sub> (0.55 mmol, 0.127 g) dissolved in 2 ml of ethanol was added. The reaction vessel was left open to the atmosphere at room temperature (ca. 23 °C) for crystallisation. Green crystals of **14** were harvested upon formation.

Synthesis of (acr)<sub>3</sub>[Zn(OH<sub>2</sub>)I<sub>2</sub>(O<sup>-i</sup>prop)] (**15**). Acridine (0.28 mmol, 0.051 g) was dissolved in 6 ml of isopropanol, after which a solution of ZnI<sub>2</sub> (0.28 mmol, 0.088 g) dissolved in 2 ml of isopropanol was added. The reaction vessel was left open to the atmosphere at room temperature (ca. 23 °C) for crystallisation. Crystals of **15** were harvested upon formation.

Found for **15**: C, 53.91; H, 3.91; N, 4.75%; calcd. for C<sub>42</sub>H<sub>37</sub>N<sub>3</sub>O<sub>2</sub>ZnI<sub>2</sub>: C, 53.95; H, 3.99; N, 4.49%.

Synthesis of (acr)<sub>3</sub>[Zn(OH<sub>2</sub>)I<sub>2</sub>(O-EtOH)] (**16**). Acridine (0.28 mmol, 0.050 g) was dissolved in 6 ml of ethanol, after which a solution of ZnI<sub>2</sub> (0.28 mmol, 0.091 g) dissolved in 2 ml of ethanol was added. The reaction vessel was left open to the atmosphere at room temperature (ca. 23 °C) for crystallisation. Crystals of **16** were harvested upon formation.

### Crystallographic studies

X-ray diffraction data for compound **12** were collected at room temperature employing a Bruker-Nonius Kappa CCD diffractometer at the X-ray Laboratory at the University of Cambridge, U.K. The X-ray diffraction data for all the other compounds were collected using a Bruker D8 Venture diffractometer, with a Photon 100 CMOS detector, at 293(2) K, employing a combination of  $\phi$  and  $\omega$  scans. Data collections were performed at 293(2) K to

avoid temperature-dependent polymorphic transitions. Monochromatic MoK $\alpha$  radiation with a wavelength  $\lambda$  of 0.71073 Å, from an I $\mu$ S source, was used as the irradiation source. Data reduction and absorption corrections were performed using SAINT+<sup>21</sup> and SADABS<sup>22</sup> as part of the APEX II<sup>23</sup> suite. The structures were solved by direct methods using SHELXS-97,<sup>24</sup> as part of the WinGX<sup>25</sup> suite. Structure refinements were carried out using SHELXL<sup>24</sup> in WinGX<sup>25</sup> as GUI. Non-hydrogen atoms were refined anisotropically. Hydrogen atoms on aromatic ring carbon atoms were placed geometrically using a riding model, with a C–H distance of 0.930 Å. The positions of the acidic N–H hydrogens were found in the difference Fourier synthesis and placed accordingly. Free refinements of the acidic N–H hydrogen atoms were implemented. The coordinates of the hydrogen atoms on the water molecules in the compounds were calculated using the computer program “CALC-OH”, developed by M. Nardelli,<sup>19</sup> as incorporated in the WinGX<sup>25</sup> suite. Graphics and publication materials were generated using ORTEP,<sup>25</sup> PLATON<sup>17</sup> and Mercury 3.5.<sup>20</sup>

## Acknowledgements

The authors would like to thank Peet van Rooyen and Dave Liles for assistance with the crystallographic aspects of this study. CS gratefully acknowledges the National Research Foundation for financial support through an Innovation Scholarship (SFH20100706000011827). MR acknowledges financial support from the University of Pretoria and the National Research Foundation (Grant No. 87659).

## References

1. G. A. Bowmaker, S. I. Rahajoe, B. W. Skelton and A. H. White, *Z. Anorg. Allg. Chem.*, 2011, 637, 1361
2. C. Slabbert and M. Rademeyer, *CrystEngComm*, 2015, 17, 9070–9096
3. F. R. Allen, *Acta Crystallogr., Sect. B: Struct. Sci.*, 2002, 58, 380
4. Y. Cui, D. Long, W. Chen and J. Huang, *Acta Crystallogr., Sect. C: Cryst. Struct. Commun.*, 1998, 54, 1605
5. W. Wang, X. Zhang, D. Huang, H. Zhu, C. Chen and Q. Liu, *Acta Crystallogr., Sect. E: Struct. Rep. Online*, 2001, 57, m561
6. J. Valdés-Martínez, O. Muñoz and R. A. Toscano, *Acta Crystallogr., Sect. E: Struct. Rep. Online*, 2005, 61, m1590
7. B. M. E. Markowitz, M. M. Turnbull and F. F. Awwadi, *Acta Crystallogr., Sect. E: Struct. Rep. Online*, 2007, 63, m2043
8. W. L. Steffen and G. J. Palenik, *Acta Crystallogr., Sect. B: Struct. Crystallogr. Cryst. Chem.*, 1976, 32, 298
9. R. Blachnik, H. Eickmeier, M. Gather and H. Reuter, *Z. Kristallogr. - New Cryst. Struct.*, 2000, 215, 93
10. C. A. Grapperhaus, T. Tuntulani, J. H. Reibenspies and M. Y. Darensbourg, *Inorg. Chem.*, 1998, 37, 4052
11. J. F. Le Querler, M. M. Borel and A. Leclaire, *Acta Crystallogr., Sect. B: Struct. Crystallogr. Cryst. Chem.*, 1977, 33, 2299
12. H. Zhang and L. Fang, *Acta Crystallogr., Sect. E: Struct. Rep. Online*, 2005, 61, m101
13. C. Hu, Q. Li and U. Englert, *CrystEngComm*, 2003, 5, 519
14. A. J. Canty, C. L. Raston, B. W. Skelton and A. H. White, *J. Chem. Soc., Dalton Trans.*, 1982, 15

15. K. Wozniak, B. Kariuki and W. Jones, *Acta Crystallogr., Sect. C: Cryst. Struct. Commun.*, 1991, 47, 1113
16. M. C. Etter, *Acc. Chem. Res.*, 1990, 23, 120
17. A. L. Spek, *Acta Crystallogr., Sect. D: Biol. Crystallogr.*, 2009, 65, 148
18. C. A. Hunter, K. R. Lawson, J. Perkins and C. J. Urch, *J. Chem. Soc., Perkin Trans. 2*, 2001, 651
19. M. Nardelli, *J. Appl. Crystallogr.*, 1999, 32, 563
20. C. F. Macrae, P. R. Edgington, P. McCabe, E. Pidcock, G. P. Shields, R. Taylor, M. Towler and J. van de Streek, *J. Appl. Crystallogr.*, 2006, 39, 453
21. Bruker, SAINT+, Bruker AXS Inc., Madison, Wisconsin, USA, 2007
22. G. M. Sheldrick, SADABS, University of Göttingen, Germany, 1996
23. Bruker, APEX II, Bruker AXS Inc., Madison, Wisconsin, USA, 2013
24. G. M. Sheldrick, *Acta Crystallogr., Sect. A: Found. Crystallogr.*, 2008, 64, 112
25. L. J. Farrugia, *J. Appl. Crystallogr.*, 2012, 45, 849
26. C. Hu and U. Englert, *CrystEngComm*, 2001, 23, 1